Thermal mitigation effects of hydroponic rooftop greening in urban areas

2018

Yoshikazu TANAKA

Contents

CHAPTER 1

Introduction

1.1. Background

The urban heat island (UHI) effect, in which urbanized areas experience higher temperatures than surrounding rural areas (Oke, 1973), is one of many phenomena caused by environmental degradation related to urbanization. For example, this effect was cited in Japan as one reason for especially high urban air temperatures that occurred during a record heat wave in August 2013; UHI effects in the Kinki and Tokai regions of south-central Japan were the strongest in the five years leading up to 2013. UHI can have a profound impact on the lives of urban residents (Zhao et al., 2014). Therefore, the improvement of urban climate has become an increasingly important social issue.

Previous research reviews of urban climate mitigation have summarized the effects of green space on temperatures and presented methods for improving urban greening and street design (Bowler et al., 2010; Gago et al., 2013). Other studies have reviewed the usage of plants on green roofs (Dvorak and Volder, 2010), the application of green roof technology (Santamouris, 2013, 2014; Qin, 2015), and the overall implementation of green roof strategies (Saadatian et al., 2013). Aleksandrowicz et al. (2017) analyzed methods for UHI mitigation and summarized current trends in urban heat island mitigation research.

In addition to mitigating their thermal environment, green roofs can provide additional benefits such as food production in urban areas (Grewal and Grewal, 2012; Whittinghill et al., 2013; Ernwein, 2014; Thomaier et al., 2014; Badami and Ramankutty, 2015), contribution to biodiversity (Ishimatsu and Ito, 2013; Orsini et al., 2014; Lin et al., 2015), effective use of rainfall (Carson et al., 2013; Lim and Jiang, 2013; Hakimdavar et al., 2014; Wong and Jim, 2014; Whittinghill et al., 2015), and beneficial impacts on human health (Dennis and James, 2017).

1.2. Study problems

Plants on green rooftops improve thermal environments by evapotranspiration, thereby reducing heat storage in building structures. Such roofs have been installed on a number of buildings in Japan. This study assessed the use of rice plants for rooftop greening using a hydroponic system to ensure effective evaporation.

The causes of high temperature in UHI areas are related to thermal balances affected by reductions in the amount of green areas and water surfaces (which decrease latent heat flux) and increases in the extent of concrete and asphalt surfaces (which increase sensible heat flux). These effects can be mitigated by improving the thermal balance of urban environments using various methods to decrease sensible heat flux and ground conductive heat flux. Plants used for green rooftops must tolerate the high temperatures and dry conditions prevalent in such environments.

It is also important to consider heat balance in terms of the effects of microclimates and building efficiency in cities. In a study focusing on observations of heat balances over green roofs, Takebayashi and Moriyama (2007) noted that the sensible heat flux of green roofs was small because most of the absorbed heat was used in evaporation. In terms of heat transfer from the atmosphere to buildings, green roofs need constant irrigation and high-transpiration vegetation (Coutts et al., 2013). Several studies have estimated the heat balance on green roofs and assessed heat transfer using evaluation models (Feng et al., 2010; Scherba et al., 2011; Tabares-Velasco and Srebric, 2012; Yaghoobian and Srebric, 2015).

Although previous studies have considered the heat flow of rooftops, few have assessed the relationships between thermal mitigation and heat balance on green roofs. It is also important to consider factors related to the mitigation effects of urban green space. For example, Onishi et al. (2010) reported a positive relationship between land surface temperature and land use/land cover when evaluating the UHI mitigation potential of greening parking lots.

1.3. Study objectives

This study aims to evaluate thermal mitigation effects of hydroponic rooftop greening in urban buildings during summer in Osaka and Kyoto, Japan. The detailed objectives are as follows:

1. To clarify the efficacy of a hydroponic rice system for mitigating thermal environment of a rooftop in summer. The results allow a quantitative clarification of the system's effects on local air and surface temperatures, as well as on the conductive heat flux. The major climatological factors influencing thermal mitigation are also discussed.
2. To investigate the relationships between mitigation indices and heat balance terms that can reveal changes in temperature around a hydroponic green roof. A model is also proposed for assessing thermal mitigation effects of a hydroponic urban greening system based on heat balance.

1.4. Thesis structure

This thesis consists of five chapters, outlined as follows.

Chapter 1 introduces the thermal mitigation effects of green roofs on urban buildings by summarizing the background, study problems, and study objectives.

Chapter 2 reviews previous research regarding monitoring and simulation studies of both thermal mitigation effects and heat balance.

Chapter 3 documents the materials and methods used in this study.

Chapter 4 presents the results of this study. The thermal mitigation effects of hydroponic green roofs could be accurately estimated from ambient air temperature and solar radiation. The effects were better explained by solar radiation than by ambient air temperature. The results also show a relationship between thermal mitigation effects and heat balance terms on hydroponic green roofs. It is revealed thermal mitigation on the hydroponic green roof based on heat balance.

Chapter 5 discusses the results of this study. Hydroponic green roofs can affect energy

flow in two ways: through the effects of evaporative cooling on the proportions of sensible heat flux and latent heat flux and through the impact of radiation shielding on conductive heat flux. In addition, the composition of heat balance terms can estimate thermal mitigation effects in green roof areas independent of the year. This principle can be used to assess the mitigation effects of urban greening on thermal environments.

Chapter 6 summarizes the conclusions of this study.

CHAPTER 2

Literature review

2.1. Introduction

Thermal mitigation methods have included reflective "cool" roofing (e.g., Jo et al., 2010), green walls (e.g., Djedjig et al., 2016; Olivieri et al., 2017), and green roofs. As some of the above studies have shown, green roofs (the establishment of living vegetation on roofing surfaces for localized climate control) are a rapidly-increasing approach to urban climate mitigation. In this literature review, I summarize previous research on rooftop greening's effects. **Table 2-1** shows the classifications and keywords related to the reviewed research. Section 2.2 summarizes monitoring and simulation studies of thermal mitigation effects. Section 2.3 summarizes monitoring and simulation studies of heat balance. Section 2.4 summarizes the collective research reviewed.

Table 2-1 The classifications and keywords related to the reviewed research.

	Temperature	Heat balance
Monitoring	Air temperature Surface temperature Substrate property Plants and irrigation Experimental platform Extent urban area Hydroponic green system	Sensible heat flux Latent heat flux Net radiation Solar radiation Seasonal changes
Simulation	Large scale urban area Microclimate change Weather Research and Forecasting model (WRF) ENVI-met model	Energy exchanges Substrate temperature Substrate moisture Plant coverage Thermal mitigation factor

2.2. Thermal mitigation from rooftop greening

2.2.1. Thermal Mitigation Monitoring

Air temperature changes depending on measurement height above the rooftop level. In one study in which air temperature was measured at three heights above a rooftop garden (0.3 m, 0.6 m, and 1 m), the maximum reduction of air temperature over the green area at 0.3 m was 4.2 °C (Wong et al., 2003). In addition, ambient air temperature near rooftop surfaces is closely related to the rooftop surface temperature: over an un-vegetated roof under dry conditions, ambient air temperature 0.3 m above the exposed substrate surface can reach 40 °C when the peak surface temperature reaches 73.4 °C (Wong et al., 2007a). Thus, in order to decrease ambient air temperature, it is important to consider methods for reducing surface temperature. Green roofs are an effective method for achieving this reduction; in Japan the surface temperature on a green roof area can decrease from 60 °C to 30 °C in fine weather and from 40 °C to 30 °C in cloudy weather (Onmura et al., 2001). In a tropical climate, the difference in surface temperature between green and bare roof areas can reach 18 °C (Wong et al., 2007b).

Plant leaves can intercept solar radiation above a roof surface, providing effective cooling (Chan and Chow, 2013). The soil covered by this canopy layer plays a role in heat storage that reduces surface temperature (Jim and Tsang, 2011). Although green roof substrates affect the heat storage and insulation of the building, it is necessary to consider the load limit of the structure with regards to the total weight of the green roof to determine whether such a system can be installed. An ideal substrate is comprised of a balance of lightweight and well-drained material (Ondono et al., 2014).

Evapotranspiration by plants mitigates the thermal environment on rooftops (Coutts et al., 2013). Suitable plants for green roofs include those in the genus Sedum, which tolerate high temperatures and dry conditions and are easy to manage (Nagase and Dunnett, 2010). Irrigation is also an important factor on green roofs. Green roofs commonly utilize plants that rely on Crassulacean acid metabolism (CAM), in which leaf pores open at night rather

than day, minimizing water loss to the atmosphere in hot or dry conditions. Such plants require less water; irrigating twice a week under tropical climate conditions provided the most thermal environment mitigation (Lin and Lin, 2011). The use of irrigation can significantly reduce air temperature during hot conditions (Broadbent et al., 2017), but when the plants are damaged by drought or mismanagement, the cooling effect is lower than that of a healthy green roof (Speak et al., 2013), making proper irrigation management necessary. In an experimental setting, a modeled small-scale green roof also decreased air temperature (Ouldboukhitine et al., 2014).

Remote sensing is another effective tool for evaluating the thermal environment in urban areas. For example, Kawashima (1991) examined the effects of vegetative density on surface temperatures in urban and suburban areas of Tokyo, based on daytime and nighttime Landsat TM imagery. The degree of vegetative effect on surface temperature depends on the relative percentage of urbanized and forested areas (Kawashima, 1994), confirming that vegetation density affects urban surface temperature. Remote-sensing-based analyses can also provide basic data for green space planning in urban areas (Sung, 2013; Kong et al., 2014).

Hydroponic systems are another approach to thermal mitigation by rooftop greening. Hydroponic green roof systems reduced rooftop temperatures and heat amplitude by 5 °C and 55%, respectively (Huang et al., 2016). The hydroponic approaches can decrease roof surface temperature as well as reduce the heat flux into the building, making it effective in mitigating thermal environments.

2.2.2. Thermal Mitigation Simulations

In large-scale urban areas, computer models are another method for assessing the thermal mitigation effect. For example, the Weather Research and Forecasting model (WRF) has been used to investigate the potential of green roof technology (Smith and Roebber, 2011), and to quantitatively evaluate the formation mechanisms of high-temperature events (Takane et al., 2013). To reduce the surface UHI by 1 °C, the Baltimore-Washington

metropolitan area (U.S.A.) needs about 30% of the total roof area to be covered by green roofs with sufficient irrigation (Li et al., 2014). Green vegetation deployment in Singapore could reduce the near-surface air temperature by more than 1 °C during nighttime when the UHI intensity is high (Li and Norford, 2016). Green roofs can have a moderate effect on the surrounding microclimate in Mediterranean-contentinal climates (Alcazar et al., 2016).

The three-dimensional microclimate model ENVI-met is another tool used for evaluating the effects of green roofs on ambient climate. For example, the effects of building density and height in urban areas were investigated in terms of the mean radiative temperature and the thermal mitigation capacity of green roofs (Perini and Magliocco, 2014). During summer in Phoenix (U.S.A.), the relationship between canopy coverage and reduction of air temperature showed a positive correlation in greened areas (Middel et al., 2015). Vegetative elements such as grass, green roofs, and trees improved the thermal comfort at pedestrian level in Bilbao, Spain (Lobaccaro and Acero, 2015). The presence of street-side trees in the central business district of Beiing, China decreased ambient air temperature by up to 0.5 °C (Wang and Zacharias, 2015). The role of green roofs in UHI mitigation in Australia was analyzed by Razzaghmanesh et al. (2016).

2.3. Heat balance

Heat balance consists of several elements (net radiation, conductive heat flux, sensible heat flux, and latent heat flux). In general, net radiation is measured by radiation sensor at the site, while conductive heat flux is measured using heat flux plates. Sensible heat flux (temperature changes without a change in phase) and latent heat flux (temperature changes involving a change in phase) are estimated from meteorological observations. The thermal conditions in the atmosphere surrounding plants and buildings can be evaluated from the heat flux composition of heat balance. One of the causes of urban climate deterioration is the decrease in latent heat flux and the increase in sensible heat flux resulting from the increase in artificial infrastructure produced by urbanization. Thus, it is important to reduce sensible heat flux as a component of the overall heat balance. This section summarizes

recent research in terms of the effects of rooftop greening on heat balance.

2.3.1. Heat Balance Monitoring

On green roof surfaces, the sensible heat flux is small because of the large latent heat flux produced by evaporation, although the net radiation is still large (Takebayashi and Moriyama, 2007). With the increasing solar reflectance of greened urban surfaces, the outflow of short-wave solar radiation increases and less solar heat energy is absorbed, leading to lower surface temperatures and reduced outflow of thermal radiation into the atmosphere (Akbari and Matthews, 2012). Thus the sensible heat flux is small on greened or reflective roofs, such that the thermal conditions are improved. Previous research has mostly focused on this process during the heat of summer, but it is necessary to conduct further studies on seasonal changes in green roof effects in other seasons. For example, on green roofs in a tropical climate, the minimum latent heat flux was recorded in January and the maximum in July (Jim and He, 2010). In a midwestern U.S. climate, green roofs consistently reduced heat fluxes in all seasons compared to gravel roofs (Getter et al., 2011).

2.3.2. Heat Balance Simulations

Analyses of incoming and outgoing energy between green roofs and the atmosphere can be important for assessing the energy balance of these systems, for example by constructing a simple but practical mathematical model (Feng et al., 2010). Scherba et al. (2011) evaluated sensible heat flux on different colors and surfaces by model simulation (validated with field experiments). The maximum sensible heat flux on reflective and green roofs was reduced by about 70% compared to a black roof. Total daily sensible heat flux was reduced by about 80% on a reflective roof and 52% on a green roof compared to a black roof. Sensible heat flux for the reflective roof was reduced by increasing albedo, while for the green roof it was reduced by increasing evapotranspiration. Studies comparing cool roofs with green roofs show that both of these approaches have beneficial thermal mitigation effects (Zinzi and Agnoli, 2012; Kolokotsa et al., 2013).

Other modeling work determined that solar radiation and medium layer moisture are major determinants of thermal insulation (Sun et al., 2013; Sun et al., 2014) and that the temperature of green roof substrate surfaces decreases with increasing plant coverage (Yaghoobian and Srebric, 2015). Suter et al. (2017) explored the urban energy balance model, finding a robust linear relationship between average latent heat flux and mean surface layer temperature reduction. Tabares-Velasco and Srebric (2012) presented a sophisticated heat and mass transfer model for green roofs that can be used to calculate substrate thermal conductivity, soil evaporation from substrate resistance, and plant transpiration.

2.4. Summary

This section reviewed recent research on the thermal mitigation and heat balance effects of green roof technology with regards to the UHI effect. Both air and surface temperature are important when considering the thermal effects of green roofs. Roof substrates also play an important role in the temperature profile of green roofs, so it is necessary to consider the depth and materials of substrates used. The cooling potential also depends on the plants and irrigation methods used; the latter can have an especially significant effect. In addition to experimental studies, modeling and remote sensing analysis can be used for assess the efficacy of green roof technology; models are most effective for evaluating the influence of green roofs on the UHI effect when the target area is the broadest. A newly-emerging approach to green roof thermal mitigation is the use of hydroponic system installed on the rooftop. This approach increases the amount of evapotranspiration and thus enhances the cooling effect; further research should continue exploring this approach.

Thermal changes in the atmosphere surrounding plants and buildings in green roof settings can also be evaluated by considering the heat balance. An especially important consideration is the need to increase latent heat flux and reduce sensible heat flux. On green surfaces, sensible heat flux is lower because of the large latent heat flux produced by evapotranspiration. Green roofs are most effective in this regard during summer heat.

Several simulations showed that the temperature decrease related to rooftop greening is partly caused by the decrease in absorbed solar radiation by the substrate surface due to canopy shading. Water bodies incorporated into green rooftops can potentially increase latent heat and heat storage in these systems.

CHAPTER 3

Materials and Methods

3.1. Site description

This study was conducted on two rooftops (in Osaka and Kyoto) for two months (62 days: 1 July to 31 August) in two consecutive years (2013 and 2014). I selected the study sites under different weather conditions. The study sites were the Osaka Gas building (34°41' 18" N, 135° 30' 01" E) and an agriculture building at Kyoto University (35° 01' 49" N, 135° 47' 07" E). Average summer conditions at the Osaka Meteorological Observatory from 1981 to 2010 were 27.4 °C in July and 28.8 °C in August. Precipitation was 157 mm in July and 91 mm in August. Potential evapotranspiration calculated by the Thornthwaite method was 187 mm in July and 195 mm in August. The average summer conditions at the Kyoto Meteorological Observatory from 1981 to 2010 were 26.8 °C in July and 28.2 °C in August. Precipitation was 220 mm in July and 132 mm in August. Potential evapotranspiration calculated by the Thornthwaite method was 176 mm in July and 167 mm in August.

3.2. Hydroponic green system

The hydroponic green system used in this study compromised a circulatory system with three open pools and two tanks, all made from polyethylene (thickness 3 mm, specific heat capacity 2.3 J g^{-1} K^{-1}) (**Fig. 3-1**). Three hydroponic systems were installed in an area of approximately 25 m^2. Water in the system was pumped from the downstream tank to the upstream tank and then returned by gravity to the lower tank, flowing in series through the three pools in which the rice was growing. The downstream tank was equipped with a float switch so that fresh water was automatically supplied to the tank whenever the water level declined below a set point.

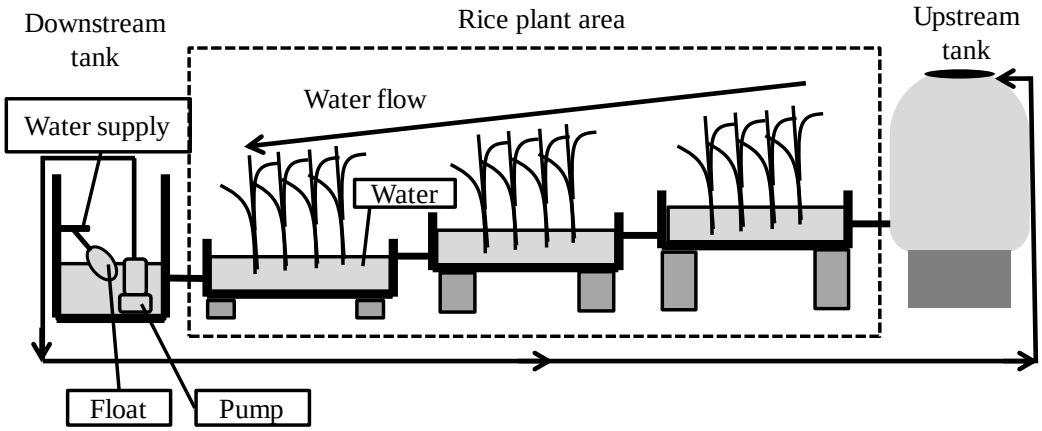

Fig. 3-1 The hydroponic green system

Table 3-1 Compositions of the nutritive liquid mixtures

NL1	Density (mmol L^{-1})	NL2	Density (mmol L^{-1})	NL3	Density (mol L^{-1})
$(NH_4)_2SO_4$	0.365	FeC_6H_5O7, xH_2O	0.025	NH_4Cl	1.4
K_2SO_4	0.091	$Ca(NO_3)_2$, $4H_2O$	0.365	KNO_3	0.4
$MgSO_4$, $7H_2O$	0.547			KH_2PO_4	0.4
KNO_3	0.183			NH_4NO_3	0.4
KH_2PO_4	0.182				

Moreover, rain water was effectively used, since the downstream tank and the rice plant area were not covered. In a preliminary feasibility study (data not shown), I used non-circulating water, but found that algae grew excessively and stole the nutrients. For the growth of hydroponic rice on the rooftop, continuous water flow was necessary. Water circulation mixed materials and equalized thermal conditions, thereby avoiding thermal stagnation in specific parts of the water containers. The roof type was a flat concrete slab.

I calculated the weight that the rooftop could safely support. As the main part of the weight of the hydroponic green system is water, I limited water depth in the pools to 10 cm. At this water depth, the total weight of the hydroponic green system was about 80 kg m^{-2}, which was safe in a region without a significant snow load. The advantages of the hydroponic green system compared with roof ponds are ease of construction and removal, and flexibility of layout depending on the user needs.

The experimented set-up was conducted at the end of May. I sowed the rice (*Oryza sativa* L.) seed in a seedling box from the end of April to the end of May. The seedlings were then transplanted from the box to the hydroponic systems until the middle of June. The rice plants in the system were set at 19 cm intervals in synthetic sponge material (urethane foam U0281, Fuji Gomu Co. Ltd., Shizuoka, Japan) immobilized in wire nets in the units. The plants were fertilized with liquid fertilizer solutions (**Table 3-1**). Before transplanting, the rice seedlings were fertilized with NL1 and NL2. After transplanting, an ammonium chloride- based fertilizer (NL3) was applied to the plants weekly. The rice plants started to flower on 12 August, 80 days after transplanting. The flowering period coincided with an especially hot period. I harvested the plants on 4 October, 53 day after flowering.

During the analysis periods, the density of rice plants was about 23 plants m^{-2} and the height was about 76 cm.

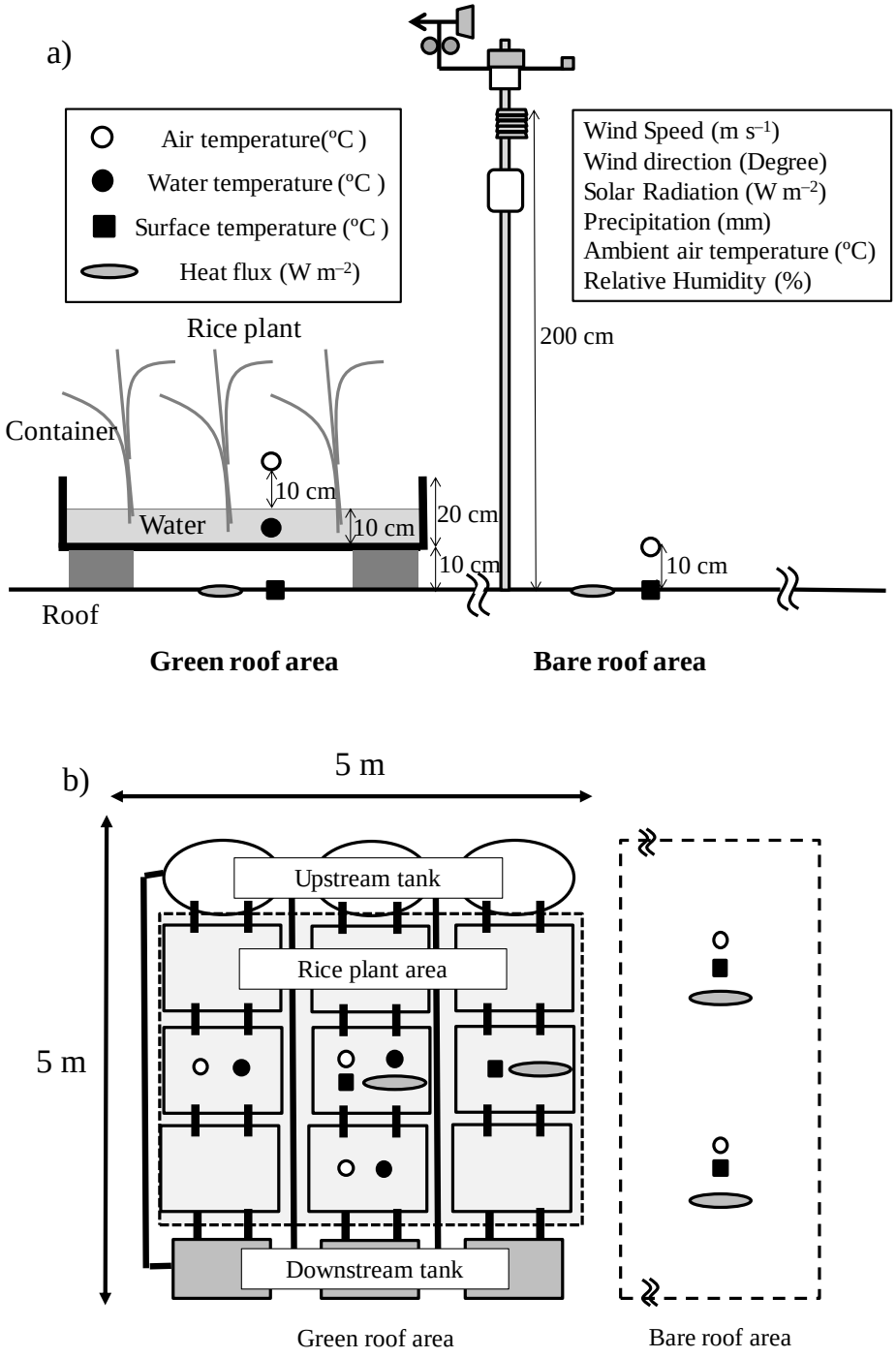

Fig. 3-2 Installation locations of sensors and instruments:
(a) Vertical arrangement and (b) spatial layout.

3.3. Micrometeorological observations

The installation locations of sensors and instruments are shown in **Fig**. **3-2**. I used a Campbell CR10X data logger (Campbell Scientific, Logan UT, USA) with a PHF-01 heat flux plate (Prede, Tokyo, Japan) and an array of thermocouples. The heat flux meter generated a small output voltage that was proportional to the temperature difference between the upper and lower surfaces of the meter. The data were recorded in the logger. Heat flux meters were attached to the roof surface with a small amount of adhesive at two points on the green roof area and two points on the bare roof area. The thermocouples had a measurement range of –200 to 300 °C. On the green roof area, they were placed at three points each to measure air temperature and water temperature, and two points to measure surface temperature. On the bare roof area, they were placed at two points each to measure air temperature and surface temperature. Air temperatures were measured 10 cm above the water surface in the green roof area and above the roof surface in the bare roof area. I observed each micrometeorological element at 12 points on the site. The data for each element were averaged prior to analysis. Weather observation systems (Onset Computer Corporation, Bourne, MA, USA) were set up at both sites. There were seven sensors located 200 cm above the surface of the roof each sensor observed ambient air temperature, relative humidity, precipitation, solar radiation, wind direction, and wind speed. The thermistor had a measurement of –40 °C to 75 °C and accuracy of ± 0.21 °C from 0 °C to 50 °C. The high-polymer humidity sensor had a measurement range of 0–100 % RH at –40 °C to 75 °C and accuracy of ± 2.5 % from 10 % to 90 % RH. The pyranometer had a measurement range of 0–1280 W m^{-2} and accuracy of ± 10 W m^{-2}. The data were observed every 30 s by a thermistor, a high-polymer humidity sensor, a tipping-bucket rain gauge, a pyranometer, a wind vane, and a three-cup anemometer, respectively. Measured data was processed and recorded in the data logger every 30 min.

3.4. Mitigation indices for air temperature, surface temperature, and conductive heat flux

In this study, I define mitigation indices, one each for air temperature, surface temperature, and conductive heat flux.

The mitigation index for air temperature (°C), is defined as

$$\Delta T_{\mathrm{A}} = T_{\mathrm{G}} - T_{\mathrm{B}} \quad (1)$$

where T_{G} is the air temperature in the green area (°C) and T_{B} the air temperature in the bare roof area (°C).

The mitigation index for surface temperature (°C), is defined as

$$\Delta T_{\mathrm{S}} = T_{\mathrm{W}} - T_{\mathrm{S}} \quad (2)$$

where T_{W} is the water temperature in the green area (°C) and T_{S} the surface temperature in the bare roof area (°C). As the water is flowing and mixed continuously in the pools, the water temperature represents the surface temperature in the green roof area. Increasingly negative values of this index correspond to larger mitigation effects on surface temperature provided by the hydroponic green system.

The mitigation index for the conductive heat flux (W m $^{-2}$) is defined as

$$\Delta G = G_{\mathrm{G}} - G_{\mathrm{B}} \quad (3)$$

where G_{G} represents the conductive heat flux in the green area (W m $^{-2}$) and G_{B} the conductive heat flux in the bare roof area (W m $^{-2}$). Increasingly negative values of this index correspond to greater mitigation effects provided by the hydroponic green system. Here, the conductive heat flux is bidirectional, assuming positive values when heat energy is transferred from the atmosphere into the building, and negative values when heat energy is

transferred from the building into the atmosphere.

I suggest two indices for expressing the mitigation effects on the green roof area and the bare roof area: air temperature and surface temperature. The mitigation index for air temperature normalized based on the air temperature in the bare roof area (NT_A, in K), is defined as:

$$NT_A = -\frac{T_G - T_B}{T_B + 273.15} \quad (4)$$

where T_B is air temperature in the bare roof area (°C).

The mitigation index for surface temperature normalized by surface temperature (NT_S, in K), is defined as:

$$NT_S = -\frac{T_W - T_S}{T_S + 273.15} \quad (5)$$

where T_W is water temperature in the green roof area (°C) and T_S surface temperature in the bare roof area (°C).

3.5. Calculation methods for factors of heat balance

3.5.1. Assessment of net radiation and downward longwave radiation

Net radiation (W m^{-2}) is defined as:

$$R_n = (1 - \alpha)S_r^{\downarrow} + L^{\downarrow} - L^{\uparrow} \quad (6)$$

where R_n is net radiation (W m^{-2}), α albedo, $S_r^{\downarrow}$ solar radiation (W m^{-2}), $L^{\downarrow}$ downward longwave radiation (W m^{-2}), and $L^{\uparrow}$ upward longwave radiation (W m^{-2}). Albedo is defined as 0.25 on the green roof area and 0.15 on the bare roof area (Tsang and Jim, 2011; Sun et

al., 2013; Lee et al., 2016).

Downward longwave radiation is defined as:

$$L^{\downarrow} = 287.7 + 2.090(T_{\mathrm{A}} + 273.15) + 2.748e \quad (7)$$

where T_{A} is ambient air temperature on the rooftop (°C) and e water vapor pressure (h Pa). Equation (7) was evaluated using air temperature and water vapor pressure during the study periods, measured by the JMA Aerological Observatory (Tateno, Japan). These were taken as representative values for Japan. Upward longwave radiation is defined as:

$$L^{\uparrow} = \varepsilon\sigma(T_{\mathrm{S}} + 273.15)^4 \quad (8)$$

where ε is emissivity, σ the Stefan–Boltzmann constant (W m^{-2} K^{-4}), and T_s surface temperature on the green roof area (°C). Surface temperature on the green roof area was defined as the water temperature in the pool.

3.5.2. Assessment of latent heat flux and water heat storage flux

Latent heat flux on the green area was estimated using the Bowen ratio method. Latent heat flux is defined as:

$$lE = \frac{R_n - G - S}{1 + \beta} \quad (9)$$

where lE is latent heat flux (W m^{-2}), R_n net radiation (W m^{-2}), G conductive heat flux (W m^{-2}), S water heat storage flux (W m^{-2}), and β the Bowen ratio. The observed data for net radiation and conductive heat flux were used in these calculations. The Bowen ratio is defined as:

$$\beta = \frac{\gamma \Delta T}{\Delta e} \quad (10)$$

where γ is the psychrometer constant (h Pa °C^{-1}), ΔT the difference between the water temperature on the green roof area and the ambient air temperature (°C), and Δe the difference in water vapor pressure between the air on the green roof area and the ambient air (h Pa).

3.6. Statistical analysis

During analysis periods, the average difference of daily air temperature performed a simple t–test. Regression analysis was used to analyze relationships between some factors and thermal mitigation indices. **Table 3-2** showed correlations (R^2 value and P value) between mitigation index and net radiation, latent heat flux, thermal mitigation factor. Thermal mitigation factor is defined later. Statistical analyses were carried out using R ver.3.3.2.

Table 3-2 Correlations (R^2 value and *P* value) between mitigation index and net radiation, latent heat flux, thermal mitigation factor.

	Mitigation index for air temperature (NT_A)	Mitigation index for surface temperature (NT_S)
Daily data		
Net radiation (W m^{-2})	R^2=0.52, p <0.05	R^2=0.68, p <0.05
Latent heat flux (W m^{-2})	R^2=0.59, p <0.05	R^2=0.71, p <0.05
Thermal mitigation factor (W m^{-2})	R^2=0.64, p <0.05	R^2=0.76, p <0.05
Hourly data		
Net radiation (W m^{-2})	R^2=0.68, p <0.05	R^2=0.75, p <0.05
Latent heat flux (W m^{-2})	R^2=0.63, p <0.05	R^2=0.65, p <0.05
Thermal mitigation factor (W m^{-2})	R^2=0.81, p <0.05	R^2=0.83, p <0.05

CHAPTER 4

Results

4.1. Weather conditions on-site

Air temperatures in the green roof and bare roof areas increased gradually until mid-August 2013 (**Fig. 4-1a**). The total precipitation for the period 1 July to 31 August 2013 was 177.2 mm, representing only 70% of the 30-year average for 1981 to 2010. Average ambient air temperature was higher than the past 30-year period. Higher values for daily mean solar radiation were recorded for the 10-day period from 9 August. The average air temperature for the two months was 28.5 ± 0.2 °C on the green roof area and 30.3 ± 0.3 °C on the bare roof area. The average difference in air temperature between the two was 1.8 °C ($p < 0.05$).

During summer 2014, air temperatures at the green roof and bare roof areas increased gradually until the end of July, and in August lower temperatures and higher precipitation were recorded than in the previous year (**Fig. 4-1b**). In 2014, from 1 July to 31 August, total precipitation was 537.9 mm, which is 1.5 times the 30-year average for 1981 to 2010. The highest integrated solar radiation (325 W m^{-2}) for the two months of this study was recorded on 26 July. Average air temperatures for the two months was 26.5 ± 0.2 °C on the green roof area, and 28.4 ± 0.4 °C on the bare roof area. The average difference in air temperatures was 1.9 °C ($p < 0.05$).

I also considered variation of air temperature in the green roof area and in the bare roof area during especially hot periods (EHP). Average daily minimum ambient air temperature was 30.5 °C, and average daily maximum ambient air temperature was 32.8 °C during the EHP of 7–22 August 2013. Average daily minimum ambient air temperature was 26.0 °C and average daily maximum ambient air temperature was 31.9 °C during the EHP of 21 July–5 August, 2014.

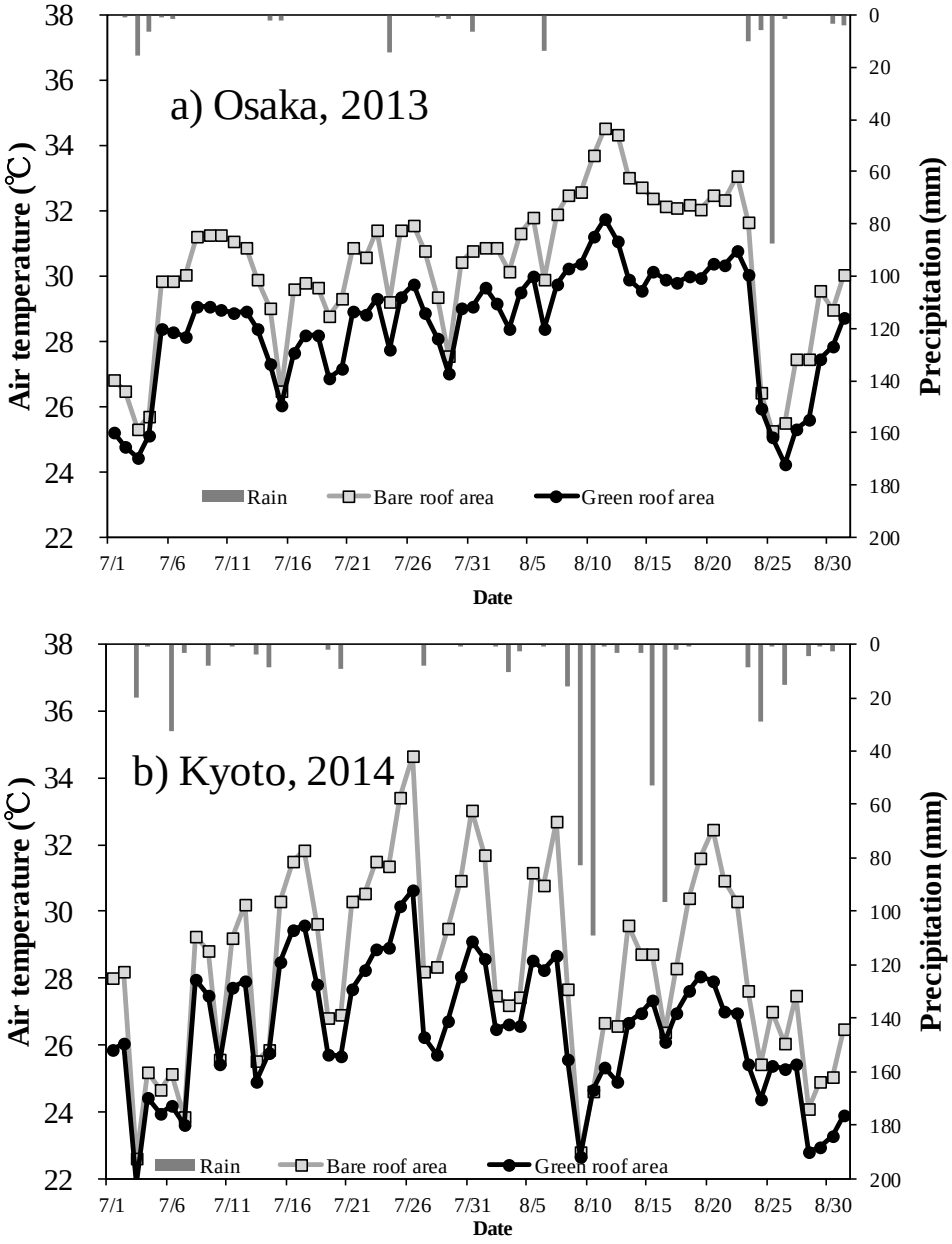

Fig 4-1 Daily average air temperature and precipitation in green roof area and bare roof area from 1 July to 31 August in (a) Osaka, 2013 and (b) Kyoto, 2014.

The mitigation effects of the hydroponic urban greening system on the thermal environment were examined using daily and hourly observation data. I used the daily data from 1 July to 31 August for 2013 and 2014, and the hourly data during the EHP. I performed regression analysis for the mitigation indices from meteorological elements observed at the experimental site. Higher coefficients of determination were found in the regressions of the mitigation indices on ambient air temperature and solar radiation. Compared with the coefficients of determination for these two elements, those on the other elements (relative humidity, water vapor pressure, wind speed, wind direction, sunshine duration, and precipitation) were lower. A possible rationale for the low coefficients of determination of the other elements might result from indirect action of these elements on the thermal environment. I also analyzed the thermal mitigation effects from heat balance elements based on the experimental data.

4.2. Mitigation effect of hydroponic green system on air temperatures

4.2.1. Mitigation effect on daily air temperature

During the experiment, daily average air temperatures exceeded 30 °C in the green and bare roof areas during a 14-day period in July and a 24-day period in August (**Fig. 4-1a**). Notably, daily average air temperature in the bare roof area exceeded 32 °C for 15 days in August. During the hottest 16-day period, from August 7 to 22, the average daily air temperature in the green roof area (30.3 °C) was 2.5 °C less than that in the bare roof area (32.8 °C).

When daily ambient air temperature rose from 22 to 33 °C, the mitigation index for air temperature improved from 0 to –4.6 °C, for an average mitigation index for air

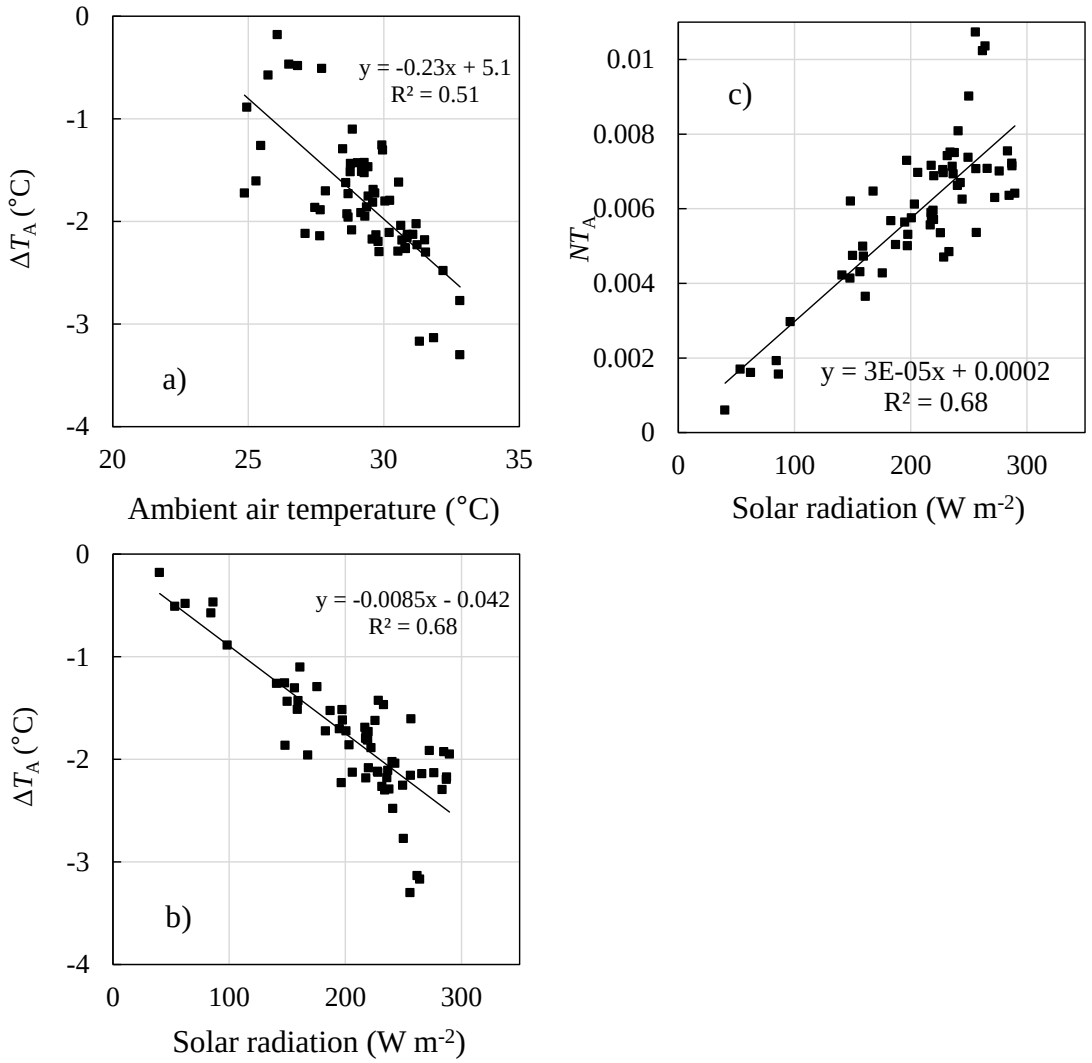

Fig. 4-2 Linear regression of the mitigation index for daily air temperature on (a) Daily ambient air temperature and (b) Daily integrated solar radiation. (c) Linear regression of the normalized mitigation index for daily air temperature on daily integrated solar radiation.

temperature of –1.8 °C for the EHP (**Fig. 4-2a**). The coefficient of determination for the regression between the mitigation index for air temperature and daily ambient air temperature was 0.51. The mitigation index for the air temperature was –2.0 °C when the daily ambient air temperature was 30 °C.

The mitigation of heating provided by the hydroponic green system also increased with increasing solar radiation (**Fig. 4-2b**). The coefficient of determination of 0.68 for the linear regression of mitigation index for air temperature on solar radiation is higher than that on daily ambient air temperature. The regression predicts that the mitigation index would improve from –1.0 to –2.5 °C as the daily mean solar radiation increases from 100 to 300 Wm^{-2}.

The normalized mitigation index for air temperature (NT_A) was proportional to the daily mean solar radiation (**Fig. 4-2c**). The y-intercept of the regression line was nearby zero. This relationship suggests that the major factor affecting the mitigation effect for air temperature provided by the hydroponic green system is the energy of solar radiation.

4.2.2. Mitigation effect on hourly air temperature

The coefficient of determination of the regression of mitigation index for air temperature on hourly ambient air temperatures during the study period was 0.77, indicating a tight relationship (**Fig. 4-3a**). The regression predicts that the mitigation index would be –1.1 °C when the hourly ambient air temperature is 30 °C, and –5.0 °C when the hourly ambient air temperature is 35 °C. The coefficient of determination of the regression of the mitigation index for air temperature on hourly integrated solar radiation is 0.74, indicating a tight relationship similar to that for the hourly ambient air temperature (**Fig. 4-3b**). The normalized mitigation index for air temperature NT_A was linearly related to the hourly solar radiation (**Fig. 4-3c**). Because the y-intercept of the regression line is not zero, it might represent the effects of elements other than solar radiation.

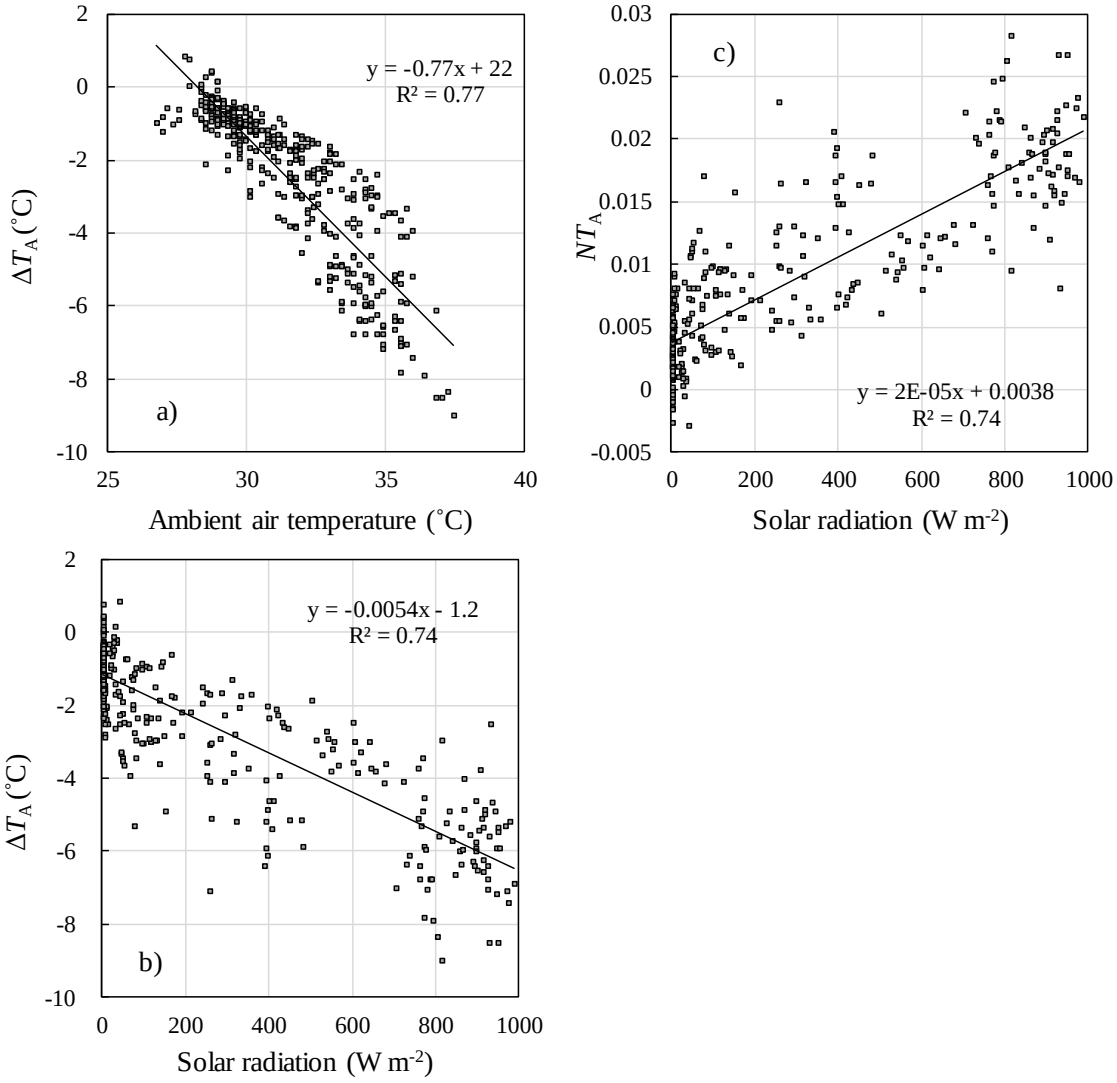

Fig. 4-3 Linear regression of the mitigation index for hourly air temperature on (a) Hourly ambient air temperature and (b) Hourly integrated solar radiation. (c) Linear regression of the normalized mitigation index for hourly air temperature on hourly integrated solar radiation.

4.3. Mitigation effect on surface temperatures

4.3.1. Mitigation effect on daily surface temperature

High surface temperatures were observed in most of July and August; however, temperatures were below 31 °C on rainy days (**Fig. 4-4**). There were two periods when the daily average surface temperature in the bare roof area exceeded 35 °C, the 5-day interval from 8 to 12 July and the 16-day interval from 7 to 22 August.

When daily ambient air temperature increased from 25 to 30 °C, the mitigation for surface temperature increased from –0.5 to –3.0 °C (**Fig. 4-5a**). The average mitigation index for surface temperature for the EHP was –3.3 °C. The coefficient of determination of a regression of the mitigation index for surface temperature on daily ambient air temperature is 0.45; the mitigation index is –3.4 °C when the daily ambient air temperature is 30 °C. The coefficient of determination for the regression of mitigation index for surface temperature on solar radiation (0.83; **Fig. 4-5b**) was even higher than that on the ambient air temperature. The regression predicts that the mitigation index would increase from –1.0 to –5.0 °C, as daily integrated solar radiation increased from 100 to 300 W m $^{-2}$.

The normalized mitigation index for surface temperature (NT_S) was linearly related to the daily mean solar radiation (**Fig. 4-5c**). The y-intercept of the regression line was negative. This relationship in the daily data means that the surface temperature in the

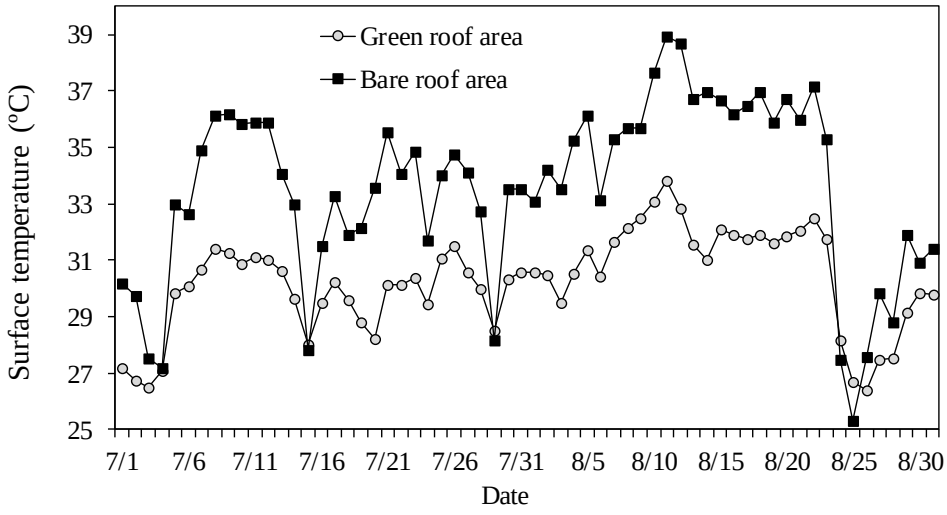

Fig. 4-4 Daily surface temperature in green and bare roof areas and daily precipitation from 1 July to 31 August 2013.

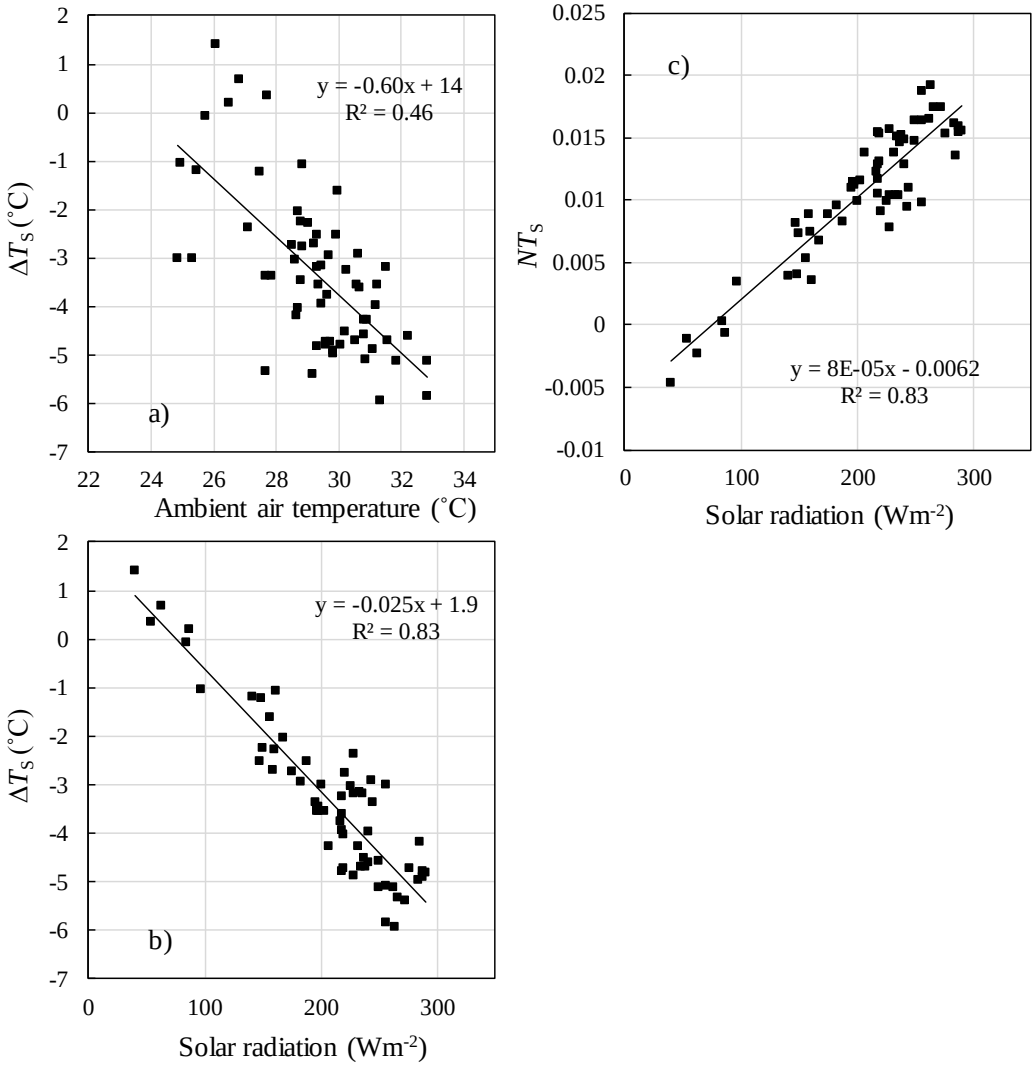

Fig. 4-5 Linear regression of the mitigation index for daily surface temperature on (a) Daily ambient air temperature and (b) Daily integrated solar radiation. (c) Linear regression of the normalized mitigation index for daily surface temperature on daily integrated solar radiation.

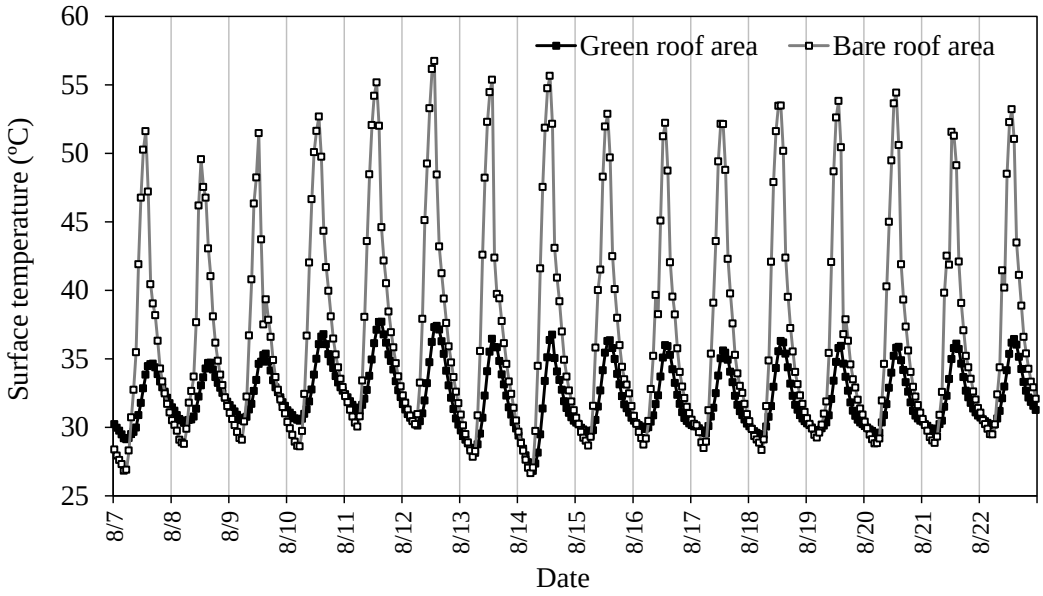

Fig. 4-6 Hourly surface temperatures in green and bare roof areas for the especially hot period (EHP) from 7 to 23 August 2013.

hydroponic green system area tended to be higher than the surface temperature on the bare roof area when the solar radiation was low. Heat storage effects of the hydroponic green system might emerge in the daily data and cause this result.

4.3.2. Mitigation effect on hourly surface temperature

During the EHP, hourly changes in the surface temperature for the green and bare roof areas were subject to especially large variations (**Fig. 4-6**): the average surface temperature during the EHP was 36.7 °C in the bare roof area, and 32.1 °C in the green roof area. In the bare roof area, surface temperature was highest (56.7 °C) between 13:00 and 14:00 on 12 August. In the green roof area, surface temperature was highest (37.7 °C) between 15:00 and 16:00 on 11 August.

The linear regression of the mitigation index for surface temperature on hourly ambient air temperature is strong (coefficient of determination 0.66; **Fig. 4-7a**). The regression predicts that the mitigation index would be –2.0 °C when the hourly ambient air temperature was 30 °C, and the mitigation index would be –12.5 °C when hourly ambient

air temperature was 35 °C. The linear regression of the mitigation index of surface temperature on hourly integrated solar radiation also is strong (coefficient of determination 0.79; **Fig. 4-7b**).

The normalized mitigation index for surface temperature (NT_S) was clearly proportional to the hourly integrated solar radiation (**Fig. 4-7c**). The y-intercept of the regression line was nearly zero. The strong regression of the normalized mitigation index on air temperature suggests both that the major factor affecting the mitigation effect provided by the hydroponic green system is the energy of solar radiation, and that the mitigation index normalized by absolute temperature is an appropriate index for estimating the cooling effect.

4.4. Mitigation effect on conductive heat flux

I observed the conductive heat flux in both the green roof area (G_G) and the bare roof area (G_B). The value of conductive heat flux is positive when heat energy flows from the atmosphere to the building. The mitigation index for conductive heat flux was estimated based on the difference in conductive heat flux into the building between the green and bare roof areas. Increasingly negative values of this index correspond to greater mitigation effects provided by the hydroponic green system.

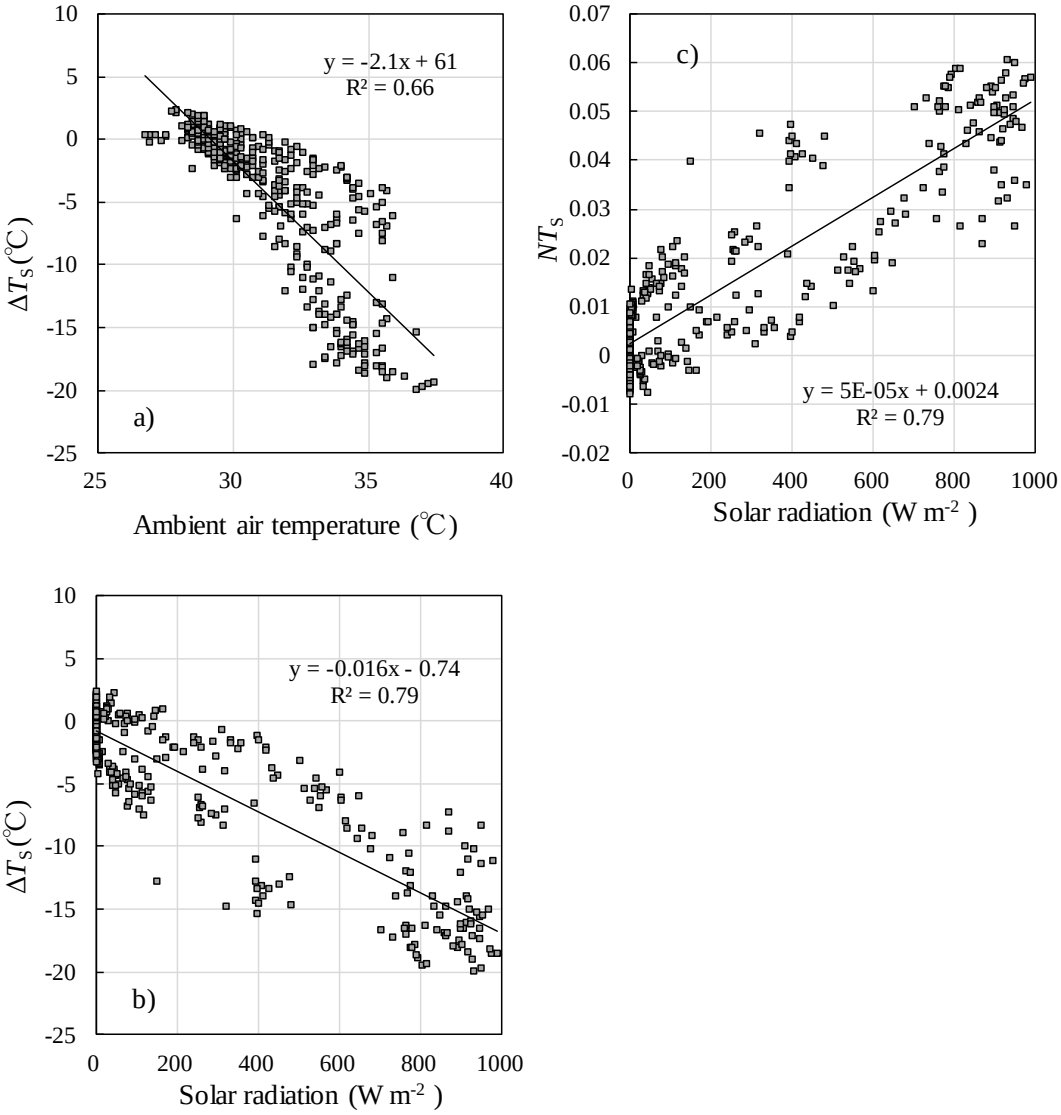

Fig. 4-7 Linear regression of the mitigation index for hourly surface temperature on (a) Hourly ambient air temperature and (b) Hourly integrated solar radiation. (c) Linear regression of the normalized mitigation index for hourly surface temperature on hourly integrated solar radiation.

4.4.1. Daily conductive heat flux

Because the daily conductive heat flux is temporally averaged for a day, the intensity of the heat load to the building in daytime and the intensity of the heat load to the atmosphere in nighttime cannot be seen from the daily accumulated conductive heat flux. The daily conductive heat flux analysis was divided into two phases to consider the directions of heat energy flow. Daily totals of heat flux for the two phases were estimated from the hourly heat flux by considering the direction of heat flow. **Fig. 4-8a** shows the daily variations in conductive heat flux into the building. Except for 5 July, the daily mean conductive heat flux for the green roof area was reduced to less than 10 W m^{-2}, compared with a range of between 20 and 60 W m^{-2} for the bare roof area. The average conductive heat flux values of 6.1 W m^{-2} for the green roof area and 42 W m^{-2} for the bare roof area during the study period indicate that conductive heat flux into the building in the green roof area was 15 % that of the bare roof area; thus, the hydroponic green system reduced the conductive heat flux by 85 %.

Conductive heat flux out from the building in the green roof area was always smaller than that in the bare roof area (**Fig. 4-8b**). The absolute value of the daily mean conductive heat flux was smaller than 13 W m^{-2} in the green roof area, compared with a range of between 0 and 64 W m^{-2} for the bare roof area. For the entire study period, the average integrated conductive heat flux values of –6.5 W m^{-2} for the green roof area and –40 W m^{-2} for the bare roof area indicate that conductive heat flux out from the building in the green roof area was 16 % that of the bare roof area; hence, the hydroponic green system reduced the conductive heat flux by 84 %.

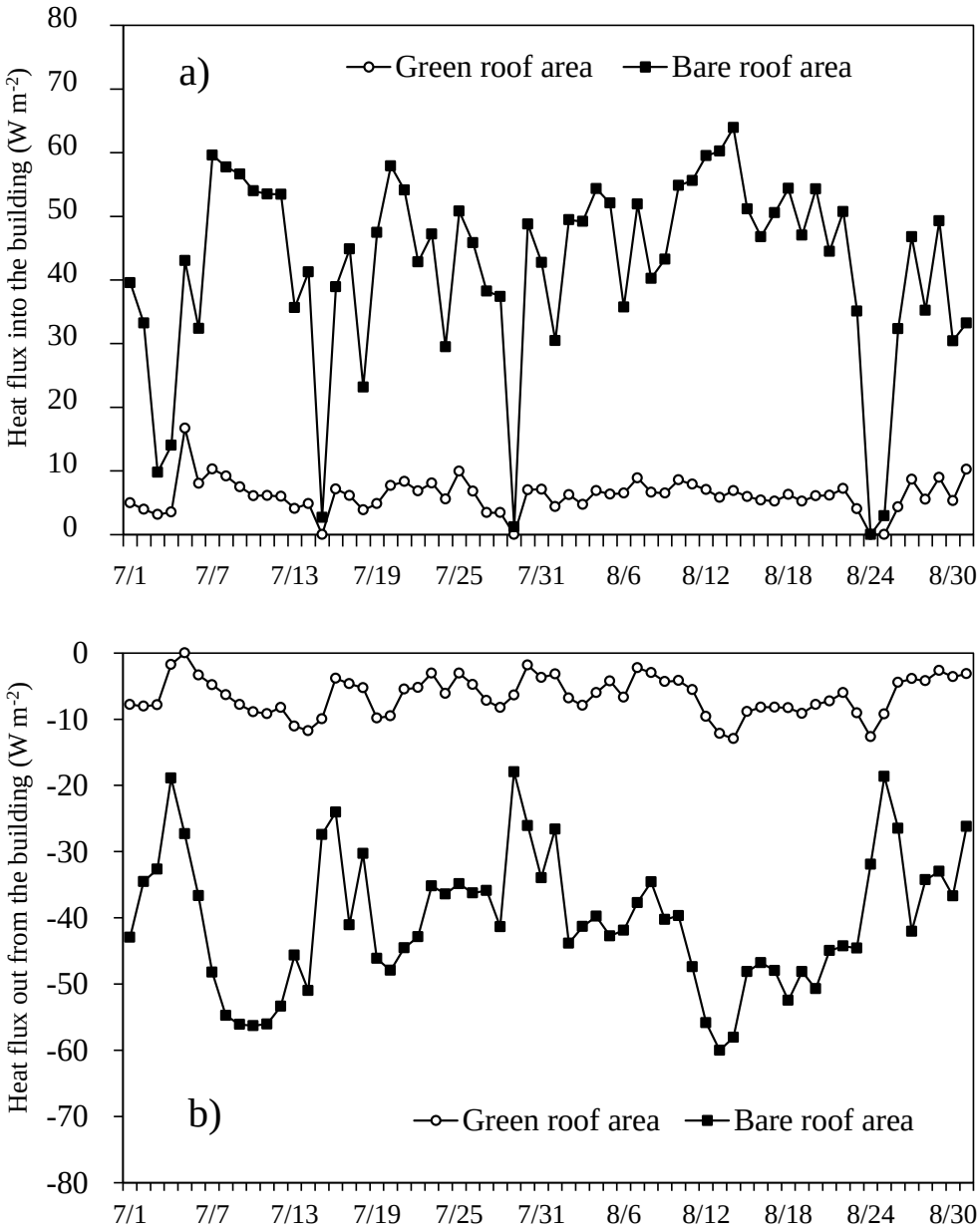

Fig. 4-8 Daily conductive heat flux in green and bare roof areas from 1 July to 31 August 2013 (a) into the building and (b) out from the building.

4.4.2. Mitigation effect on daily conductive heat flux

The relationship between conductive heat flux into the building (influx) and meteorological elements was analyzed by calculating the mitigation index for daily conductive heat flux ($=\Sigma G_{G\ in} - \Sigma G_{B\ in}$) based on the difference in conductive heat flux into the building between the green and bare roof areas. Based on regression of the mitigation index for conductive heat flux into the building on daily ambient air temperature, the coefficient of determination of 0.39 was obtained. This coefficient indicates that these two variables are related to some degree. The coefficient of determination of 0.86 obtained by regressing the mitigation index for daily conductive heat flux into the building on the daily solar radiation (**Fig. 4-9a**) indicates that the coefficient of determination of the daily solar radiation is prominently higher than that for regression on the daily ambient air temperature.

Next, the relationship between conductive heat flux out from the building (outflux) and meteorological factors was analyzed by calculating the mitigation index for daily conductive heat flux ($=\Sigma G_{G\ out} - \Sigma G_{B\ out}$) for the difference in conductive heat flux between the two rooftop areas. The regression of the mitigation index for conductive heat flux out from the building on the daily ambient air temperature yielded a coefficient of determination of 0.32, indicating that the relationship between these two variables is weak. A coefficient of determination of 0.76 was obtained by regressing the mitigation index for daily conductive heat flux out from the building on daily solar radiation (**Fig. 4-9b**). The coefficient of determination for the regression on daily solar radiation was higher than that on daily ambient air temperature.

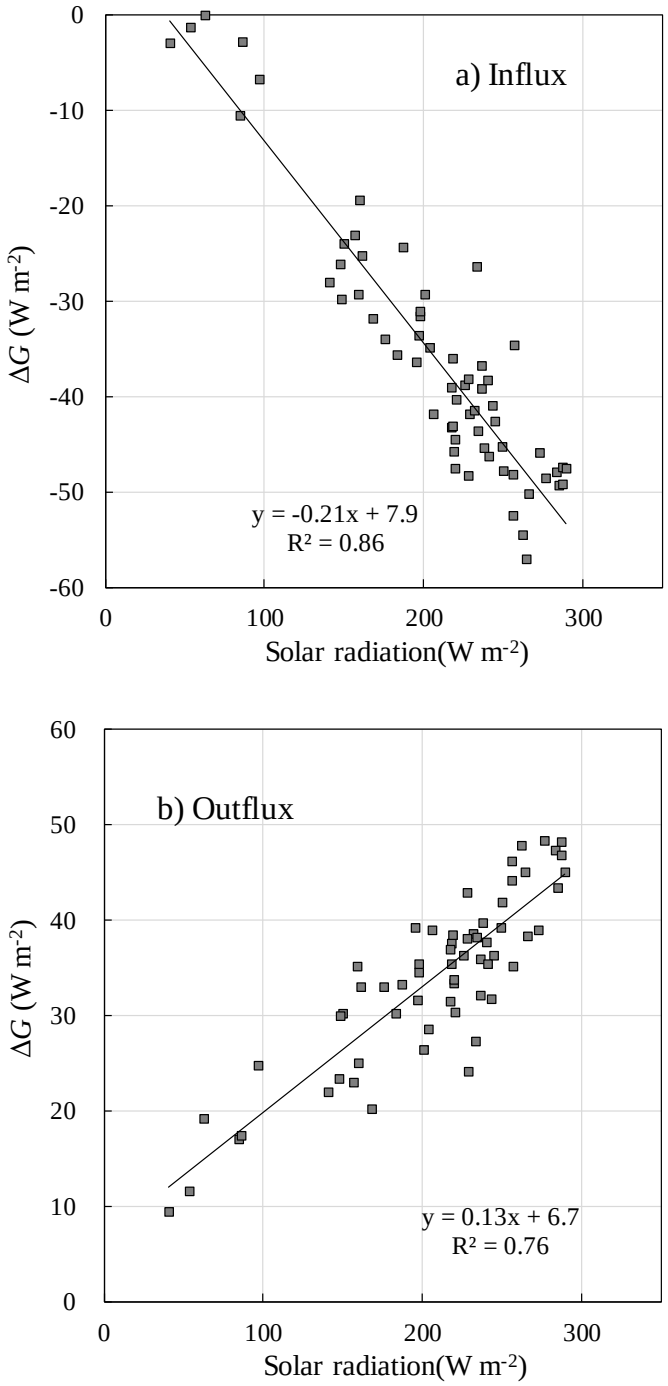

Fig. 4-9 Linear regression of the mitigation index for daily conductive heat flux on daily integrated solar radiation. (a) Conductive heat flux into the building (influx), (b) Conductive heat flux out from the building (outflux).

4.4.3. Temporal changes in hourly conductive heat flux

I studied changes in hourly conductive heat flux for the green and bare roof areas during the EHP (**Fig. 4-10**). In the green roof area, heat energy flowed into the building (positive values) from 10:00 to 18:00, but heat flowed out from the building at other times. In the bare roof area, heat energy flowed into the building from 8:00 to 14:00. In the green roof area, the maximum hourly conductive heat flux into the building was 472 W m $^{-2}$ on 14 August at 14:00, and the maximum hourly conductive heat flux out from the building was –375 W m $^{-2}$ on 14 August at 6:00. In the bare roof area, the maximum hourly conductive heat flux into the building was 3465 W m $^{-2}$ on 14 August at 11:00, and the maximum hourly conductive heat flux out from the building was –2248 W m $^{-2}$ on 19 August at 16:00. Thus, heat fluxes into and out of the building were an order of magnitude higher in the bare roof area.

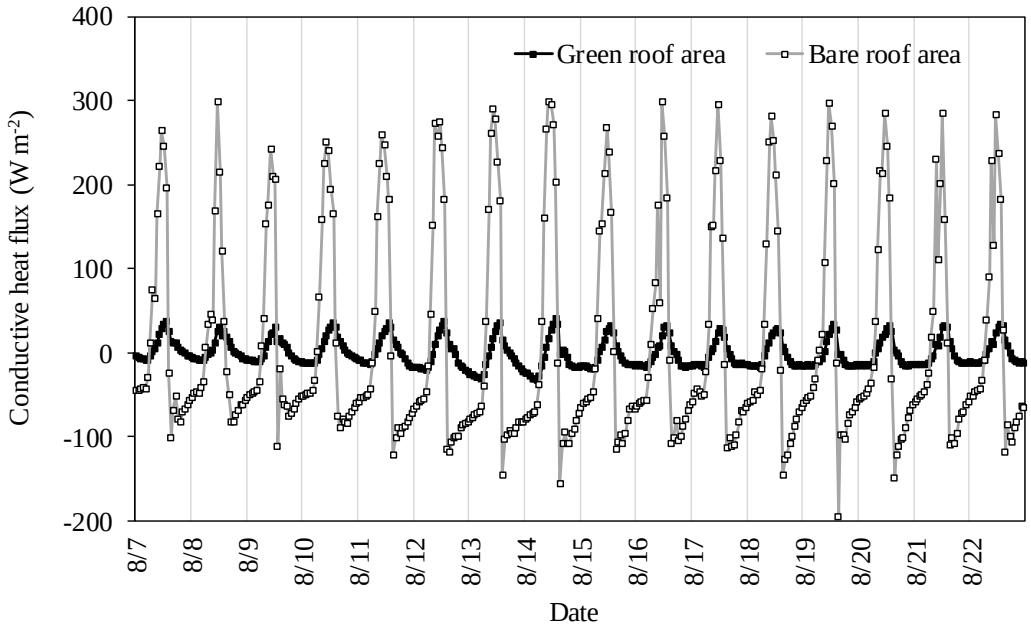

Fig. 4-10 Hourly conductive heat flux in green and bare roof areas for the especially hot period (EHP).

4.4.4. Mitigation effect on hourly conductive heat flux

I analyzed the relationships between the hourly mitigation index for conductive heat flux and ambient air temperature, using hourly data and 4 symbols, corresponding to different cases (**Fig. 4-11a**). Case1 (illustrated with □ symbols) represents positive values for both G_G and G_B (conductive heat flux in the green and bare roof areas, respectively), indicating that heat energy was flowing into the building in both the green and bare roof areas. In Case1, the hourly mitigation index for conductive heat flux was large and negative, indicating that heat influx in the green roof area was smaller than that in the bare roof area, and the mitigation effect for conductive heat flux increased as ambient air temperature increased. Case2 (illustrated with ◆ symbols) represents negative values for G_G and positive values for G_B, indicating that heat outflux occurred in the green roof area but heat influx occurred in the bare roof area. In Case2, the mitigation effect was smaller than that in Case1. Case 3 (illustrated with ∆ symbols) represents positive values of G_G and negative values of G_B, indicating that heat influx occurred in the green roof area but heat outflux occurred in the bare roof area. In Case 3, the mitigation index for conductive heat flux was positive at higher ambient air temperatures. Case 4 (illustrated with × symbols) represents negative values for both G_G and G_B, indicating that heat outflux from the building occurred in both the green and bare roof areas. In Case 4, the mitigation index for conductive heat flux was positive, indicating that outflux in the bare roof area was larger than that in the green roof area.

The relationships between solar radiation and the mitigation index for conductive heat flux are illustrated in **Fig. 4-11b**. In Case 1 (□), the hourly mitigation index for conductive heat flux was large and negative under higher solar radiation. The mitigation effect for conductive heat flux increased as solar radiation increased. The relationship between conductive heat flux and solar radiation was similar in Case 2 (◆), observed under lower solar radiation, to that in Case 1. The mitigation index for conductive heat flux in Case 3 (∆), observed under similar levels of solar radiation compared with Case2, was larger. Solar radiation in Case 4 (×) was lower, corresponding to the period from evening until the

next morning. The linear regression of the hourly mitigation index for conductive heat flux on the hourly integrated solar radiation is strong (coefficient of determination 0.79).

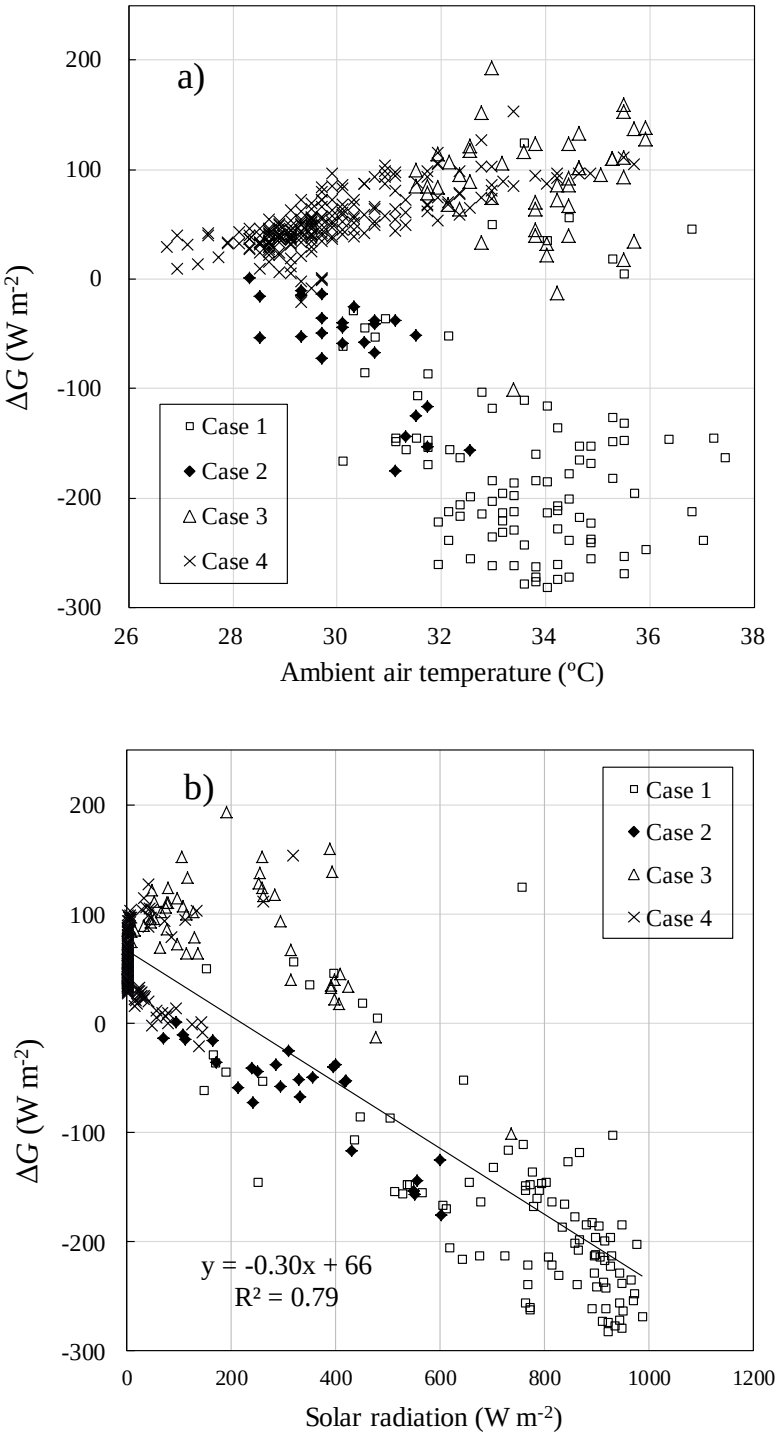

Fig. 4-11 Linear regression of the mitigation index for conductive heat flux on (a) hourly ambient air temperature and (b) hourly integrated solar radiation for the especially hot period (EHP). Case 1 (□) represents positive values for both G_G and G_B, case2 (◆) represents negative values for G_G and positive values for G_B, case 3 (△) represents positive values of G_G and negative values of G_B, case4 (×) represents negative values for both G_G and G_B.

4.5. Relationships between heat balance and thermal mitigation indices

4.5.1. Daily data

Using daily average data from 1 July to 31 August in 2013 and 2014, I showed the relationships between heat balance factor and thermal mitigation indices of the hydroponic urban greening system. **Fig. 4-12a** shows the relationships between net radiation and mitigation index for air temperature. Statistical analysis (**Table 3-2**) showed that the coefficient of determination for the regression between net radiation and the mitigation index for air temperature was 0.52 in total (0.57 for 2013 and 0.62 for 2014, $p < 0.05$). When net radiation increased, the ratio of decreasing air temperature also increased. **Fig. 4-12b** shows the relationships between net radiation and mitigation index for surface temperature. The coefficient of determination for the regression between net radiation and the mitigation index for surface temperature was 0.68 in total (0.78 for 2013 and 0.81 for 2014, $p < 0.05$). When net radiation increased, the ratio of decreasing surface temperature also increased.

Fig. 4-13a shows the relationships between latent heat flux and mitigation index for air temperature. The coefficient of determination for the regression between latent heat flux and the mitigation index for air temperature was 0.59 in total (0.61 for 2013, 0.71 for 2014, $p < 0.05$). When latent heat flux increased, the ratio of decreasing air temperature also increased. **Fig.4-13b** shows the relationships between latent heat flux and mitigation index for surface temperature. The coefficient of determination for the regression between latent heat flux and the mitigation index for surface temperature was 0.71 in total (0.81 for 2013, 0.83 for 2014, $p < 0.05$). When latent heat flux increased, the ratio of decreasing surface temperature also increased.

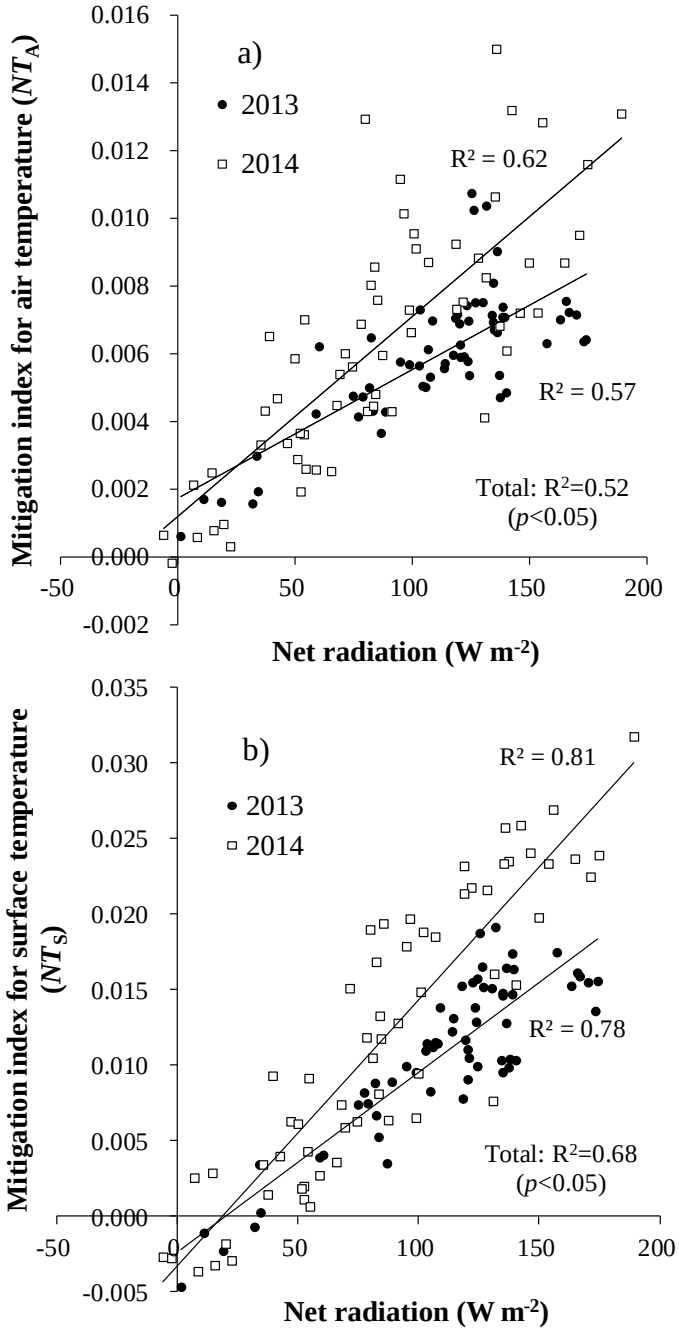

Fig. 4-12 (a) Linear regression of the daily mitigation index for air temperature on net radiation (Total: $R^2 = 0.52$, $p < 0.05$, y = 5E−05x + 0.0016); (b) Linear regression of the daily mitigation index for surface temperature on net radiation (Total: $R^2 = 0.68$, $p < 0.05$, y = 0.0001x − 0.0023).

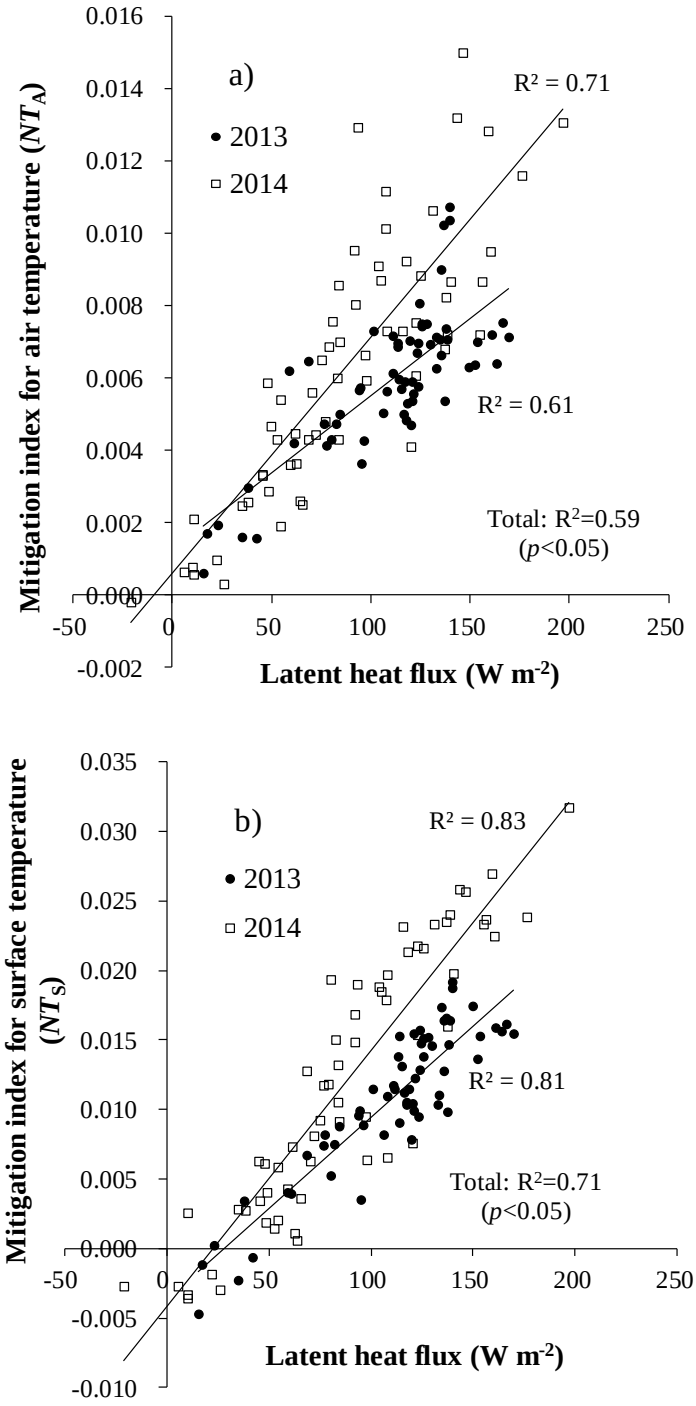

Fig. 4-13 (a) Linear regression of the daily mitigation index for air temperature on latent heat flux (Total: R^2 = 0.59, p < 0.05, y = 5E–05x + 0.001); (b) Linear regression of the daily mitigation index for surface temperature on latent heat flux (Total: R^2 = 0.71, p < 0.05, y = 0.0001x – 0.0034).

4.5.2. Hourly data during especially hot periods (EHPs)

I conducted regression analysis for the mitigation indices from heat balance elements during the EHPs in 2013 and 2014. **Fig. 4-14a** shows the relationships between net radiation and mitigation index for air temperature. The coefficient of determination of the regression of mitigation index for air temperatures during the EHP was 0.68 in total (0.69 for 2013 and 0.68 for 2014, $p < 0.05$), indicating a strong relationship. The more the net radiation increased, the larger was the ratio of decreasing air temperature. **Fig. 4-14b** shows the relationships between net radiation and mitigation index for surface temperature. The coefficient of determination of the regression of mitigation index for surface temperatures during the EHPs was 0.75 in total (0.75 for 2013 and 0.80 for 2014, $p < 0.05$), indicating a strong relationship. The more the net radiation increased, the larger was the ratio of decreasing surface temperature.

Fig. 4-15a shows the relationships between latent heat flux and mitigation index for air temperature. The coefficient of determination of the regression of mitigation index for air temperature during the EHPs was 0.63 in total (0.67 for 2013 and 0.59 for 2014, $p < 0.05$), indicating a strong relationship. The more the latent heat flux increased, the larger was the ratio of decreasing air temperature.

Fig. 4-15b shows the relationships between latent heat flux and mitigation index for surface temperature. The coefficient of determination of the regression of mitigation index for surface temperature during the EHPs was 0.65 in total (0.73 in 2013 and 0.62 in 2014, $p < 0.05$), indicating a strong relationship. The more the latent heat flux increased, the larger was the ratio of decreasing surface temperature.

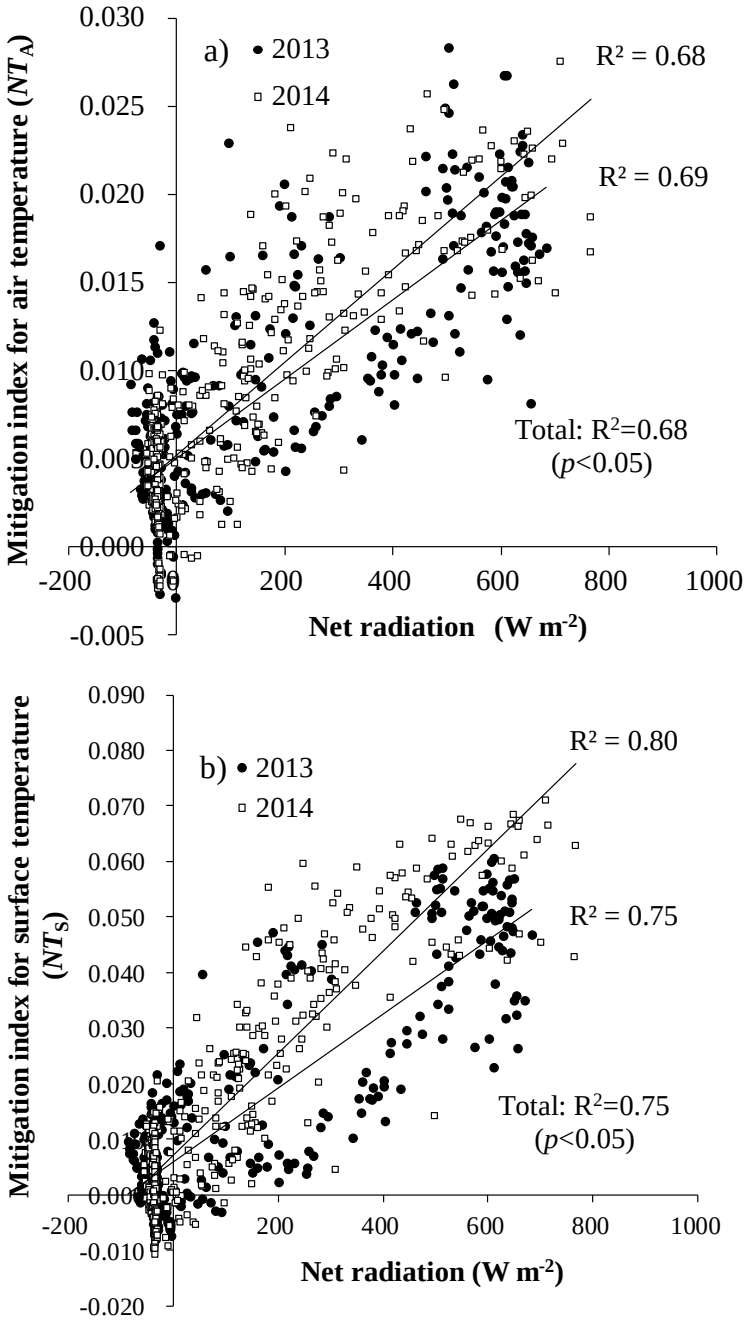

Fig. 4-14 (a) Linear regression of the hourly mitigation index for air temperature on net radiation (Total: $R^2 = 0.68$, $p < 0.05$, y = 2E−05x + 0.0051); (b) Linear regression of the hourly mitigation index for surface temperature on net radiation (Total: $R^2 = 0.75$, $p < 0.05$, y = 8E−05x + 0.0066).

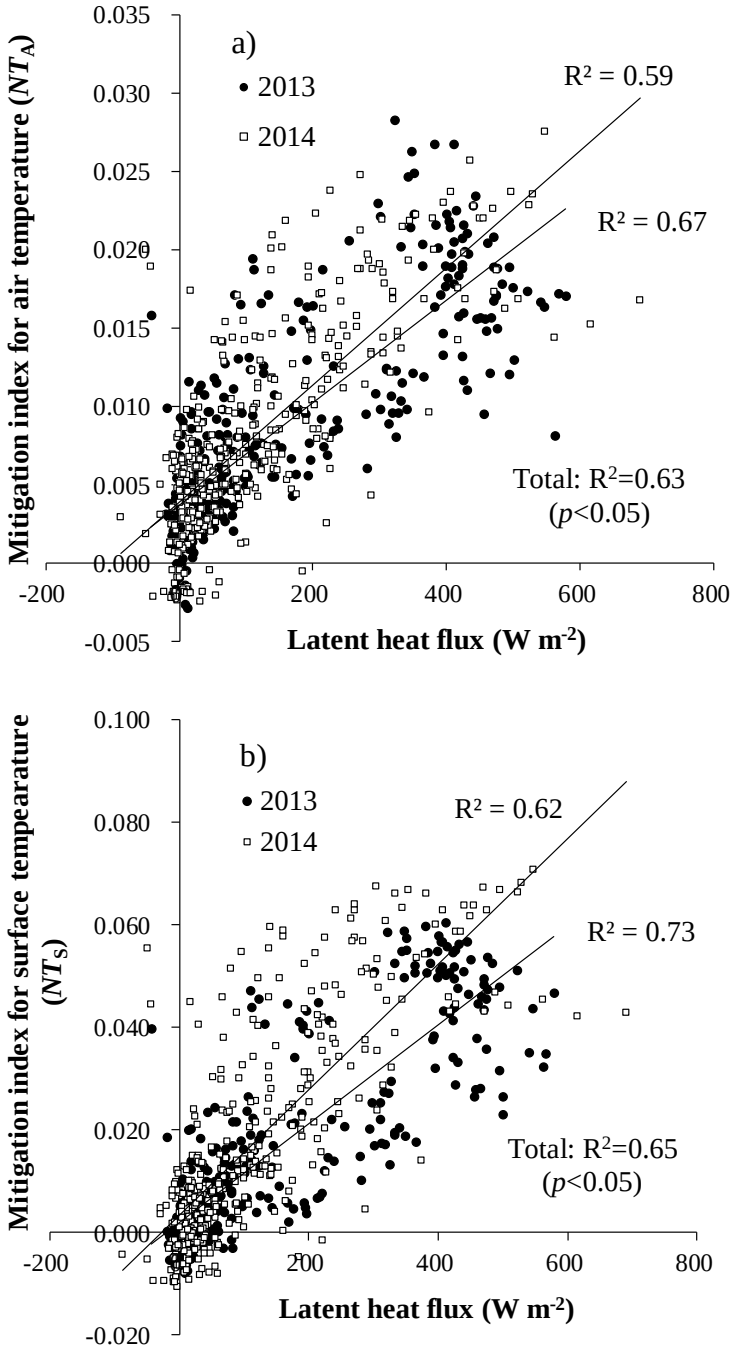

Fig. 4-15 (a) Linear regression of the hourly mitigation index for air temperature on latent heat flux (Total: R^2 = 0.63, p < 0.05, y = 3E–05x + 0.0038); (b) Linear regression of the hourly mitigation index for surface temperature on latent heat flux (Total: R^2 = 0.65, p < 0.05, y = 0.0001x + 0.003).

CHAPTER 5

Discussion

5.1. Mitigation of temperature by rooftop hydroponic green system

This study clarified the mitigation effects by a rooftop hydroponic green system on air temperature, surface temperature, and conductive heat flux. During the EHP (7-22 August), the average air temperature in the bare roof area was about 32.8 °C and the average air temperature in the green roof area was about 30.3 °C, for a mitigation effect of 2.5 °C. Getter et al. (2011) indicated that heat transfer and thermal differences between green roofs and gravel roofs appear to be primarily influenced by solar radiation, ambient air temperature, and volumetric moisture content of the growing medium. Increasing the water content of roof surfaces increases the amount of evapotranspiration, which decreases air temperature. In this study, the green roof area occupied by the hydroponic green system was always flooded with water, causing active evapotranspiration that I conjecture was directly responsible for evaporative cooling that decreased the air temperature. The coefficient of determination of 0.51 for the regression of the mitigation index for air temperature on daily ambient air temperature indicates a strong linear relationship between these variables. The coefficient of determination of 0.68 for the regression of the mitigation index for air temperature on daily integrated solar radiation indicates an even stronger relationship. Thus, I conclude that solar radiation was the dominant factor that affected the mitigation of increasing air temperatures, due to increases in the evapotranspiration from the hydroponic green system.

High surface and air temperatures in the bare roof area were observed throughout the study period; the relative lack of rain compared with the previous year may have contributed to the record high temperatures of 2013. For the EHP, I observed an average

mitigation index for surface temperature of –3.3 °C. Meng and Hu (2005) reported the evaporative cooling of moist, porous medium: the surface temperature of the wet medium was 25 °C lower than that of dry roof with no such media. In this study, the mitigation index for hourly surface temperature was –20 °C when the solar radiation was around 1000 W m^{-2}. Lin and Lin (2011) reported a surface temperature of 33.1 °C in a green roof area and 35.5 °C in the adjacent bare roof area when crassulacean acid metabolism (CAM) plants were used, for a temperature difference of 2.4 °C. They suggested the rooftop greening with C4 plants (C4 carbon fixation) provides greater mitigation of surface temperatures than that provided by CAM plants. I found the coefficient of determination of 0.83 for regression of the mitigation effect on surface temperature on daily solar radiation. Solar radiation affected the mitigation of increasing surface temperature due to evapotranspiration from the hydroponic green system and the interception of solar radiation by the hydroponic green system.

5.2. Mitigation of conductive heat flux by rooftop hydroponic green system

Analysis of the conductive heat flux on the Osaka Gas building rooftop showed that heat flux in the green roof area during daytime was substantially reduced, to 15 % of that in the bare roof area; heat outflux in the green roof area during nighttime was reduced to 16 % of that in the bare roof area for the analyzed summer period. Wong et al. (2007) reported that observed heat influx on a tropical rooftop can be reduced by up to 60 % through the use of green plants. Mitigation of thermal environments by hydroponic systems is thought to be greater than those of greening methods using soil. The integrated heat outflux in the green roof area was reduced to 16 % of that in the bare roof area, due to the reduction of conductive heat flux by the storage of heat energy in tank water and the increase in latent heat flux provided by the hydroponic green system. In the bare roof area, considerable heat energy is stored in the building structure during daytime hours and released during the night. In the green roof area, less heat energy is stored in the building structure, so less heat energy is released during the night.

Coutts et al. (2013) reports that sensible heat flux is reduced when Sedum on a green rooftop is irrigated, since sensible heat flux is increased compared with that during a dry period. Indeed, my work here also demonstrates that irrigation increases evapotranspiration, which reduces both heat influx and heat outflux. Based on the relationships between meteorological elements and the mitigation index for conductive heat flux, I conjecture that heat flux into the building during daytime was reduced due to both the cooling effect of the latent heat flux from the water in the hydroponic green roof, and the interception of solar radiation by the system. Concerning hourly conductive heat flux during the EHP, heat influx in the bare roof area attained maximum values around noon. When heat influx was reduced at that time of day, the storage of heat energy in the rooftop of the building was also reduced. One of the important methods for combating urban heat island effects is to reduce heat influx during daytime.

5.3. Assessment model for thermal mitigation indices in terms of heat balance of the green area

The results section showed the methods by which the thermal mitigation indices were evaluated in terms of latent heat flux of the green area (**Figs.4-13** and **4-15**). When only the latent heat flux was used to assess the thermal mitigation indices, it was difficult to provide a uniform evaluation method for 2013 and 2014.

The difference in the heat balance between green roof and bare roof areas is related to factors such as latent heat flux, conductive heat flux, and water heat storage flux. In order to uniformly evaluate thermal mitigation on the different rooftops and to improve the accuracy of the regression model, I proposed assessment methods for thermal mitigation indices that included these three factors. I defined the thermal mitigation factor as the sum of the three heat balance factors (latent heat flux, conductive heat flux, and water heat storage flux).

5.3.1. Assessment model for daily data

I considered the assessment methods for thermal mitigation effects in different years and

sites in relation to new factors. Using the daily variations from 1 July to 31 August in 2013 and 2014, I defined the thermal mitigation factor as the sum of the heat balance terms, related closely to the thermal mitigation effects. It was considered that the conductive heat flux of the rooftop affected its surface temperature. When I defined the thermal mitigation factor, only the daily data were used for the conductive heat flux into the building. **Fig. 5-1a** shows the relationships between thermal mitigation factor and mitigation index for air temperature, with coefficient of determination of 0.64 in total (0.46 for 2013 and 0.73 for 2014, $p < 0.05$). The accuracy was improved compared to the former thermal mitigation factors (**Fig. 4-12a** and **Fig. 4-13a**). Perini and Magliocco (2014) measured mean radiant temperature and reported that the cooling effect varies depending on the amount of green areas and vegetation types. In this study, air temperature on the green roof area was measured at 10 cm above the water surface. Reductions in air temperature may vary depending on the growth stage of rice plants.

Fig. 5-1b shows the relationships between thermal mitigation factor and mitigation index for surface temperature. The coefficient of determination of the regression was 0.76 in total (0.68 for 2013 and 0.81 for 2014, $p < 0.05$). Accuracy was improved compared to the former thermal mitigation factors (**Fig. 4-12b** and **Fig. 4-13b**). Huang et al. (2016) reported that a water depth of 10 cm was sufficient to provide an ideal hydroponic green roof system that reduced rooftop temperature by 5 °C and heat amplitude by 55 %. This study also showed that water contributed to reducing the surface temperature. It is thought that the surface temperature and water heat flux varies depending on the water depth.

Thermal mitigation effects on green rooftop varied according to weather conditions and differed from those of the bare roof surface. Findings concerning the thermal environment can be difficult to translate into an urban greening strategy. Consequently, the use of the proposed assessment model provides a simple method for evaluating how the green roof influences thermal mitigation.

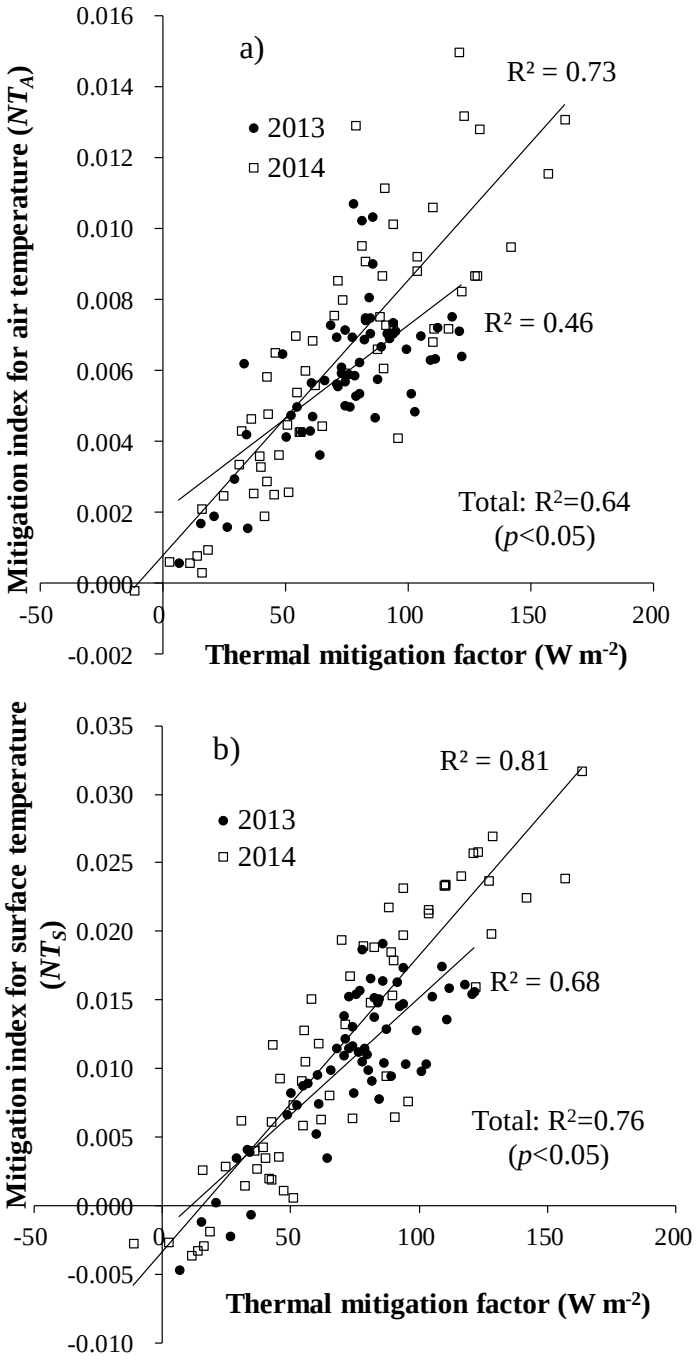

Fig. 5-1 (a) Linear regression of the daily mitigation index for air temperature on thermal mitigation factor (Total: R^2 = 0.64, p < 0.05, y = 7E−05x + 0.001); (b) Linear regression of the daily mitigation index for surface temperature on thermal mitigation factor (Total: R^2 = 0.76, p < 0.05, y = 0.0002x − 0.0033).

5.3.2. Assessment model for hourly data

In hourly data, I also considered the thermal mitigation factor as the sum of the heat balance terms related closely to the thermal mitigation effects. For short-term assessment, I must consider the time lag for equilibrium assumption. The positive daily thermal budget suggests that whether peak air temperature occurs before or after peak surface temperature depends on the combination of solar radiation, heat convection, and thermal irradiation (Qin and Hiller, 2011). In order to consider the time lag due to thermal inertia in heat balance, I calculated a moving average for the hourly data, and considered the relationship between the thermal mitigation factor and mitigation index for air temperature. When using a three-hour average, **Fig. 5-2a** shows the relationships between the thermal mitigation factor and the mitigation index for air temperature. Linear regression showed a strong relationship between the mitigation index for air temperature and the thermal mitigation factor (coefficients of determination: 0.84 for 2013, 0.79 for 2014, and 0.81 in total; $p < 0.05$; the coefficient of determination was improved compared with those in **Figs. 4-14a** and **4-15a**). Given the study conditions, it takes approximately 3 hours for heat to be transferred and to affect the rooftop air temperature. Moreover, the presence of the water storage tanks delays the transfer of heat to the rooftop, thereby both delaying the onset and reducing the maximum air temperature.

The change in conductive heat flux is reflected in the surface temperature with some phase lag. On a cement concrete surface, thermal conduction and solar absorption have approximately the same phase while the surface temperature exhibits some phase lag behind the other two (Qin, 2016). I averaged the surface temperature during the overall period, and considered the relationship between the thermal mitigation factor and the mitigation index for surface temperature. When using a three-hour average, **Fig. 5-2b** shows the relationships between the thermal mitigation factor and the mitigation index for surface temperature. Linear regression showed a very strong relationship between the mitigation index for surface temperature and thermal mitigation factor (coefficient of determination 0.86 for 2013, 0.83 for 2014, and 0.83 in total; $p < 0.05$; the coefficient of determination was

improved compared with those in **Figs. 4-14b** and **4-15b**).

In this study, since surface temperature on the green roof area was treated as water temperature, it seemed that a delay of three hours occurred as heat transfer lag. This is thought to fluctuate depending on the water depth of the hydroponic system. Furthermore, it is necessary to correct the data for varying water depth. The thermal characteristics of the observation site are generally evaluated via heat balance, as this reflects changes in the thermal environment. Considering the heat balance on the green rooftop, it was found that the thermal mitigation effect could be uniformly evaluated even for data measuring different rooftop conditions and different years. The regression model presented here provides a simple method for predicting the thermal mitigation effects of a green roof including water surface, thereby helping to set the optimum approach to rooftop greening of urban buildings.

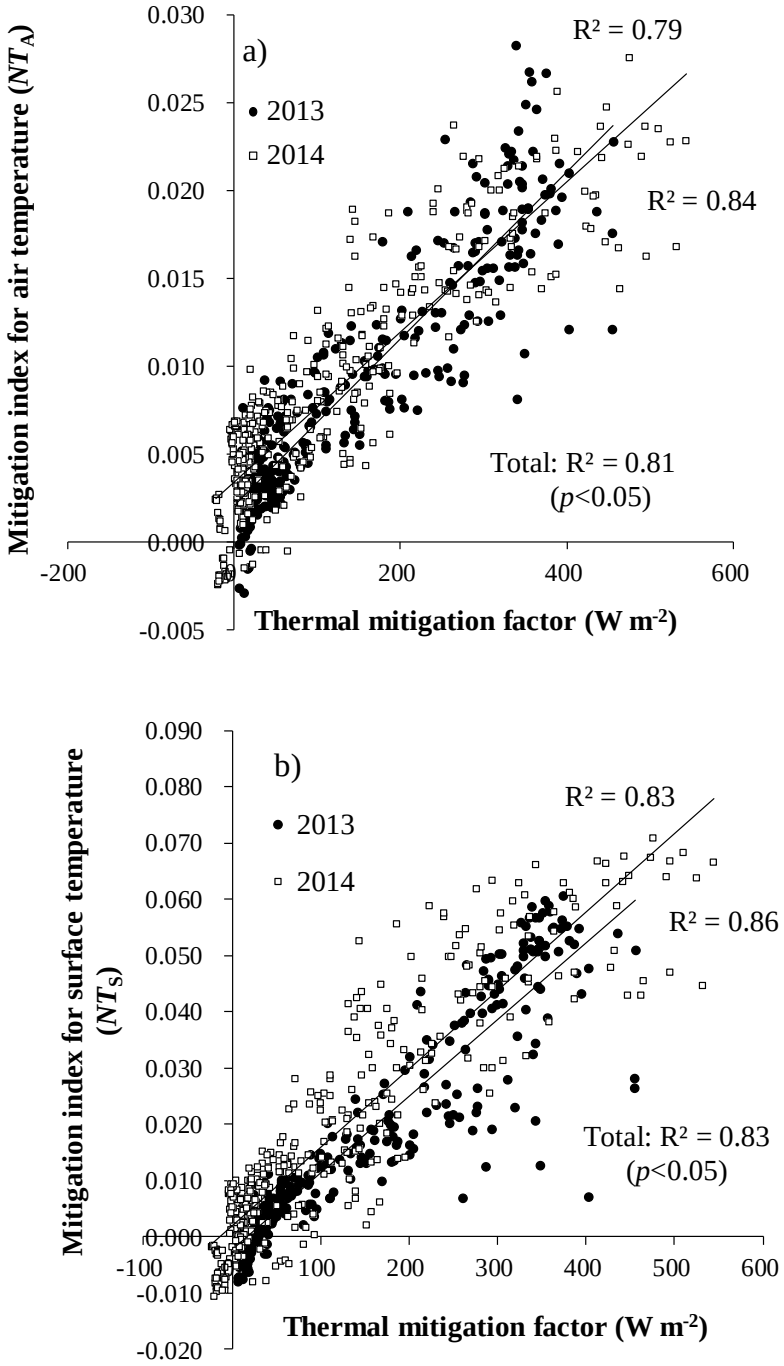

Fig. 5-2 (a) Linear regression of the hourly mitigation index for air temperature on thermal mitigation factor (Total: $R^2 = 0.81$, $p < 0.05$, y = 4E–05x + 0.0028); (b) Linear regression of the hourly mitigation index for surface temperature on thermal mitigation factor (Total: $R^2 = 0.83$, $p < 0.05$, y = 0.0001x – 0.0002).

CHAPTER 6

Conclusions

The mitigation of UHI effects by hydroponic green roof systems is greatly enhanced by the direct evaporation of water, whereas other vegetation-based green roof systems benefit from evapotranspiration occurring only from interactions between vegetation and soil moisture. The most important property of the hydroponic green system is that the leaves of plants (such as rice) act like the heat exchanger plates in air conditioners through transpiration. The results of this study agree with the principle that, given a wet surface, if more energy is supplied the cooling effect from evapotranspiration will be stronger (Penman, 1948; Monteith, 1981; Brutsaert, 2005). Although other ambient meteorological factors (e.g., wind speed or precipitation) are less significantly correlated with the mitigation indices, it is important to further investigate these to understand their roles in the entire mitigation process.

First, I clarified the effects of a hydroponic green system on the thermal environment of an urban rooftop, including consideration of the influence of weather conditions. Although the mechanisms responsible for this influence were not analyzed, I considered the relationships between standard meteorological factors and measured data, along with the influence of certain meteorological factors on the rooftop environment. The results suggested that solar radiation is a primary factor for estimating the mitigation effects of the hydroponic greening method. This solar radiation could be used for forecasting the economic benefits of hydroponic green systems.

Second, I investigated the cooling mechanism using a heat balance model that simulates the effect of a hydroponic green system on the thermal environment. The results showed the relative heat balance properties of green and bare roof areas. I defined a thermal

mitigation factor based on the heat balance and proposed an assessment model for the thermal mitigation indices. The results confirmed that the assessment model was able to estimate the thermal mitigation effects in terms of heat balance, independent of year, suggesting that solar radiation and net radiation are factors in the thermal mitigation effects of green roof areas. When using other heat balance elements to consider the thermal mitigation effect, latent heat flux was an important factor for more precise estimations of thermal mitigation. However, latent heat flux was not enough to exceed the effects.

I tried to present the effects of green roof areas using a new thermal mitigation factor that included latent heat flux, water heat storage flux, and conductive heat flux. During especially hot periods, three-hour average values were best for evaluating thermal mitigation in order to accommodate the time lag needed for heat energy to be conducted under the roof. Regarding daily variations in the analyzed terms, the data from 2013 and 2014 showed almost the same relationships between thermal mitigation factors and thermal mitigation indices of the green roof area. These results suggest a principle for assessing the mitigation effects of urban greening on the thermal environment in urban areas.

The presence of water and plants in a hydroponic system might be expected to not only mitigate the urban thermal environment, but also to provide additional benefits such as food production, contribution to biodiversity, and effective use of rainfall. I will continue to study these mitigation effects, paying attention to the multiple potential roles of urban rooftops.

Acknowledgement

This research conducted while I belonged to Graduate School of Agriculture, Kyoto University.

I am deeply grateful to Professor Dr. Shigeto KAWASHIMA, Graduate School of Agriculture, Kyoto University, for helping me the path of researching and chairperson of the examination committee of this thesis. I would like to thank to Professor Dr. Satoshi HOSHINO and Professor Dr. Masayuki FUJIHARA, Graduate School of Agriculture, Kyoto University, for becoming the member of the examination committee. I would like to offer my thanks to Associate Professor Dr. Kimihito NAKAMURA, Graduate School of Agriculture, Kyoto University, for his effective discussions and scientific comments throughout my research work. I am grateful thanks to Associate Professor Dr. Takehide HAMA, Center for Water Cycle, Marine Environment and Disaster Mitigation, Kumamoto University, for his valuable guidance, suggestions and scientific comments throughout my research work. I would like to thank to Osaka Gas Co., Ltd. for providing the research site. I would like to thank to Professor Dr. Yutaka OKUMOTO, Graduate School of Agriculture, Kyoto University, for providing rice seeds and suggesting for glowing rice plants. I have plenty of thanks to all members of Hydrological Environment Engineering Laboratory for all the good and rough times we shared and for their sincere corporation.

Finally, I have lovely thanks to my family for all supporting and warm heart.

March, 2018

Yoshikazu TANAKA

References

Akbari, H., Matthews, H.D., 2012. Global cooling updates: Reflective roofs and pavements. Energy Build. 55, 2–6. https://doi.org/10.1016/j.enbuild.2012.02.055

Alcazar, S.S., Olivieri, F., Neila, J., 2016. Green roofs: Experimental and analytical study of its potential for urban microclimate regulation in Mediterranean-continental climates. Urban Clim. 17, 304–317. https://doi.org/10.1016/j.uclim.2016.02.004

Aleksandrowicz, O., Vuckovic, M., Kiesel, K., Mahdavi, A., 2017. Current trends in urban heat island mitigation research: Observation based on a comprehensive research repository. Urban Clim. 21, 1–26. http://dx.doi.org/10.1016/j.uclim.2017.04.002

Badami, M.G., Ramankutty, N., 2015. Urban agriculture and food security: a critique based on an assessment of urban land constraints. Glob. Food Secur. 4, 8–15. https://doi.org/10.1016/j.gfs.2014.10.003

Bowler, D.E., Buyung-Ali, L., Knight, T.M., Pullin, A.S., 2010. Urban greening to cool towns and cities: A systematic review of the empirical evidence. Landsc. Urban Plan. 97, 147–155. https://doi.org/10.1016/j.landurbplan.2010.05.006

Broadbent, A.M., Coutts, A.M., Tapper, N.J., Demuzere, M., 2017. The cooling effect of irrigation on urban microclimate during heatwave conditions. Urban Clim. http://dx.doi.org/10.1016/j.uclim.2017.05.002

Brutsaert, W., 2005. Hydrology: an Introduction, Cambrige University Press, New York.

Carson, T.B., Marasco, D.E., Culligan, P.J., McGillis, W.R., 2013. Hydrological performance of extensive green roofs in New York City: observations and multi-year modeling of three full-scale systems. Environ. Res. Lett. 8, 1–13. http://dx.doi.org/10.1088/1748-9326/8/2/024036

Chan, A.L.S., Chow, T.T., 2013. Energy and economic performance of green roof system under future climate conditions in Hong Kong. Energy Build. 64, 182–198. https://doi.org/10.1016/j.enbuild.2013.05.015

Coutts, A.M., Daly, E., Beringer, J., Tapper, N.J., 2013. Assessing practical measures to reduce urban heat: green and cool roofs. Build. Environ. 70, 266–276. https://doi.org/10.1016/j.buildenv.2013.08.021

Dennis, M., James, P., 2017. Evaluating the relative influence on population health of domestic gardens and green space along a rural-urban gradient. Landsc. Urban Plan. 157, 343–351. https://doi.org/10.1016/j.landurbplan.2016.08.009

Djedjig, R., Bozonnet, E., Belarbi, R., 2016. Modeling green wall interactions with street canyons for building energy simulation in urban context. Urban Clim. 16, 75–85. https://doi.org/10.1016/j.uclim.2015.12.003

Dvorak, B., Volder, A., 2010. Green roof vegetation for North American ecoregions: A literature review. Landsc. Urban Plan. 96, 197–213. https://doi.org/10.1016/j.landurbplan.2010.04.009

Ernwein, M., 2014. Framing urban gardening and agriculture: on space, scale and the public. Geoforum 56, 77–86. https://doi.org/10.1016/j.geoforum.2014.06.016

Feng, C., Meng, Q., Zhang, Y., 2010. Theoretical and experimental analysis of the energy balance of extensive green roofs. Energy Build. 42(6), 959–965. https://doi.org/10.1016/j.enbuild.2009.12.014

Gago, E.J., Roldan, J., Pacheco-Torres, R., Ordoñez, J., 2013. The city and urban heat islands: A review of strategies to mitigate adverse effects. Renew. Sustain. Energy Rev. 25, 749–758. https://doi.org/10.1016/j.rser.2013.05.057

Getter, K.L., Rowe, D.B., Andersen, J.A., Wichman, I.S., 2011. Seasonal heat flux properties of an extensive green roof in an Midwestern U.S. climate. Energy Build. 43, 3548–3557. https://doi.org/10.1016/j.enbuild.2011.09.018

Grewal S.S., Grewal P.S., 2012. Can cities become self-reliant in food? Cities 29, 1–11. https://doi.org/10.1016/j.cities.2011.06.003

Hakimdavar, R., Culligan, P.J., Finazzi, M., Barontini, S., 2014. Scale dynamics of extensive green roofs: quantifying the effect of drainage area and rainfall characteristics on observed and modeled green roof hydrologic performance. Ecol.

Eng. 73, 494–508. https://doi.org/10.1016/j.ecoleng.2014.09.080

Huang, Y.-Y., Chen, C.-T., Tsai, Y.-C., 2016. Reduction of temperatures and temperature fluctions by hydroponic green roofs in a subtropical urban climate. Energy Build. 129, 174–185. https://doi.org/10.1016/j.enbuild.2016.07.023

Ishimatsu, K., Ito, K., 2013. Brown/biodiverse roofs: a conservation action for threatened brownfields to support urban biodiversity. Landsc. Ecol. Eng. 9, 299–304. https://doi.org/10.1007/s11355-011-0186-8

Jim, C.Y., He, H., 2010. Coupling heat flux dynamics with meteorological conditions in the green roof ecosystem, Ecol. Eng. 36, 1052–1063. https://doi.org/10.1016/j.ecoleng.2010.04.018

Jim, C.Y., Tsang, S.W., 2011. Biophysical properties and thermal performance of an intensive green roof. Build. Environ. 46, 1263–1274. https://doi.org/10.1016/j.buildenv.2010.12.013

Jo, J.H., Carlson, J.D., Golden, J.S., Bryan, H., 2010. An integrated empirical and modeling methodology for analyzing solar reflective roof technologies on commercial buildings. Build. Environ. 45, 453–460. https://doi.org/10.1016/j.buildenv.2009.07.001

Kawashima, S., 1991. Effect of vegetation on surface temperature in urban and suburban areas in winter. Energy Build. 15-16, 465–469. https://doi.org/10.1016/0378-7788(90)90022-B

Kawashima, S., 1994. Relation between vegetation, surface temperature and surface composition in the Tokyo region during winter, Remote Sens. Environ. 50 (1), 52–60. https://doi.org/10.1016/0034-4257(94)90094-9

Kolokotsa, D., Santamouris, M., Zerefos, S.C., 2013. Green and cool roofs' urban heat island mitigation potential in European climates for office buildings under free floating conditions. Sol. Energy 95, 118–130. https://doi.org/10.1016/j.solener.2013.06.001

Kong, F., Yin, H., Wang, C., Cavan, G., James, P., 2014. A satellite image-based analysis of factors contributing to the green-space cool island intensity on a city scale. Urban For. Urban Green. 13, 846–853. https://doi.org/10.1016/j.ufug.2014.09.009

Lee, H., Mayer, H., Chen, L., 2016. Contribution of trees and grass lands to the mitigation of human heat stress in a residential district of Freiburg, Southwest Germany. Landsc. Urban Plan. 148, 37–50. https://doi.org/10.1016/j.landurbplan.2015.12.004

Li, D., Bou-Zeid, E., Oppenheimer, M., 2014. The effectiveness of cool and green roofs as urban heat island mitigation strategies. Environ. Res. Lett. 9(5), 055002.

Li, X.-X., Norford, L.K., 2016. Evaluation of cool roof and vegetations in mitigating urban heat island in a tropical city, Singapore. Urban Clim. 16, 59–74. https://doi.org/10.1016/j.uclim.2015.12.002

Lim, K.-Y., Jiang, S.C., 2013. Reevaluation of health risk benchmark for sustainable water practice through risk analysis of rooftop-harvested rainwater. Water Res. 47, 7273–7286. https://doi.org/10.1016/j.watres.2013.09.059

Lin, B.B., Philpott, S.M., Jha, S., 2015. The future of urban agriculture and biodiversity-ecosystem services: Challenges and next steps. Basic Appl. Ecol. 16, 189–201. https://doi.org/10.1016/j.baae.2015.01.005

Lin, Y.-J., Lin, H.-T., 2011. Thermal performance of different planting substrates and irrigation frequencies in extensive tropical rooftop greeneries. Build. Environ. 46, 345–355. https://doi.org/10.1016/j.buildenv.2010.07.027

Lobaccaro, G., Acero, J.A., 2015. Comparative analysis of green actions to improve outdoor thermal comfort inside typical urban street canyons. Urban Clim. 14, 251–267. https://doi.org/10.1016/j.uclim.2015.10.002

Meng, Q., Hu, W., 2005. Roof cooling effect with humid porous medium, Energy Build. 37, 1–9. https://doi.org/10.1016/j.enbuild.2003.11.004

Middel, A., Chhetri, N., Quay, R., 2015. Urban forestry and cool roofs: Assessment of heat mitigation strategies in Phoenix residential neighborhoods. Urban For. Urban Green. 14, 178–186. https://doi.org/10.1016/j.ufug.2014.09.010

Monteith, J.L., 1981. Evaporation and surface temperature, Q.J.R. Meteorol. Soc. 107, 1–27.

Nagase, A., Dunnett, N., 2010. Drought tolerance in different vegetation types for extensive

green roofs: effects of watering and diversity. Landsc. Urban Plan. 97, 318–327. https://doi.org/10.1016/j.landurbplan.2010.07.005

Oke, T.R., 1973. City size and the urban heat island. Atmos. Environ. 7, 769–779. https://doi.org/10.1016/0004-6981(73)90140-6

Olivieri, F., Grifoni, R.C., Redondas, D., Sanchez-Resendiz, J.A., Tascini, S., 2017. An experimental method to quantitatively analyse the effect of thermal insulation thickness on the summer performance of a vertical green wall. Energy Build. 150, 132–148. https://doi.org/10.1016/j.enbuild.2017.05.068

Ondono, S., Bastida, F., Moreno, J.L., 2014. Microbiological and biochemical properties of artificial substrates: A preliminary study of its application as Technosols or as a basis in Green Roof Systems. Ecol. Eng. 70, 189–199. https://doi.org/10.1016/j.ecoleng.2014.05.003

Onmura, S., Matsumoto, M., Hokoi, S., 2001. Study on evaporative cooling effect of roof lawn gardens. Energy Build. 33, 653–666. https://doi.org/10.1016/S0378-7788(00)00134-1

Orsini, F., Gasperi, D., Marchetti, L., Piovene, C., Draghetti, S., Ramazzotti, S., Bazzocchi, G., Gianquinto, G., 2014. Exploring the production capacity of rooftop gardens (RTGs) in urban agriculture: the potential impact on food and nutrition security, biodiversity and other ecosystem services in the city of Bologna. Food Secur. 6, 781–792. https://doi.org/10.1007/s12571-014-0389-6

Ouldboukhitine, S.-E., Belarbi, R., Sailor, D.J., 2014. Experimental and numerical investigation of urban street canyons to evaluate the impact of green roof inside and outside buildings. Appl. Energy 114, 273–282. https://doi.org/10.1016/j.apenergy.2013.09.073

Penman, H.L., 1948. Natural evaporation from open water, bare soil and grass, Proc. R. Soc. Lond. A 193, 120–145.

Perini, K., Magliocco, A., 2014. Effects of vegetation, urban density, building height, and atmospheric conditions on local temperatures and thermal comfort. Urban For. Urban

Green. 13, 495–506. https://doi.org/10.1016/j.ufug.2014.03.003

Qin, Y., Hiller, J.E., 2011. Modeling temperature distribution in rigid pavement slabs: impact of air temperature. Constr. Build. Mater. 25, 3753–3761. https://doi.org/10.1016/j.conbuildmat.2011.04.015

Qin, Y., 2015. A review on the development of cool pavements to mitigate urban heat island effect. Renew. Sustain. Energy Rev. 52, 445–459. https://doi.org/10.1016/j.rser.2015.07.177

Qin, Y., 2016. Pavement surface maximum temperature increases linearly with solar absorption and reciprocal thermal inertial. Int. J. Heat Mass Transf. 97, 391–399. https://doi.org/10.1016/j.ijheatmasstransfer.2016.02.032

Razzaghmanesh, M., Beecham, S., Salemi, T., 2016. The role of green roofs in mitigating Urban Heat Island effects in the metropolitan area of Adelaide, South Australia. Urban For. Urban Green. 25, 89–102. https://doi.org/10.1016/j.ufug.2015.11.013

Saadatian, O., Sopian, K., Salleh, E., Lim, C.H., Riffat, S., Saadatian, E., Toudeshki, A., Sulaiman, M.Y., 2013. A review of energy aspects of green roofs. Renew. Sustain Energy Rev. 23, 155–168. https://doi.org/10.1016/j.rser.2013.02.022

Santamouris, M., 2013. Using cool pavements as a mitigation strategy to fight urban heat island- A review of the actual developments. Renew. Sustain. Energy Rev. 26, 224–240. https://doi.org/10.1016/j.rser.2013.05.047

Santamouris, M., 2014. Cooling the cities-A review of reflective and green roof mitigation technologies to fight heat island and improve comfort in urban environments. Solar Energy 103, 682–703. https://doi.org/10.1016/j.solener.2012.07.003

Scherba, A., Sailor, D.J., Rosentiel, T.N., Wamser, C.C., 2011. Modeling impacts of roof reflectivity, integrated photovoltaic panels and green roof systems on sensible heat flux into the urban environment. Build. Environ. 46, 2542–2551. https://doi.org/10.1016/j.buildenv.2011.06.012

Smith, K.R., Roebber, P.J., 2011. Green roof mitigation potential for a proxy future climate scenario in Chicago, Illinois. J. Appl. Meteorol. Climatol. 50, 507–522.

https://doi.org/10.1175/2010JAMC2337.1

Speak, A.F., Rothwell, J.J., Lindley, S.J., Smith, C.L., 2013. Reduction of the urban cooling effects of an intensive green roof due to vegetation damage. Urban Clim. 3, 40–55. https://doi.org/10.1016/j.uclim.2013.01.001

Sun, T., Bou-Zeid, E.,Wang, Z.H., Zerba, E., Ni, G.H., 2013. Hydrometeorological determinants of green roof performance via a vertically-resolved model for heat and water transport. Build. Environ. 60, 211–224. https://doi.org/10.1016/j.buildenv.2012.10.018

Sun, T., Bou-Zeid, E., Ni, G.H., 2014. To irrigate or not to irrigate: Analysis of green roof performance via a vertically-resolved hygrothermal model. Build. Environ. 73, 127–137. https://doi.org/10.1016/j.buildenv.2013.12.004

Sung, C.Y., 2013. Mitigating surface urban heat island by a tree protection policy: A case study of The Woodland, Texas, USA. Urban For. Urban Green. 12, 474–480. https://doi.org/10.1016/j.ufug.2013.05.009

Suter, I., Maksimovic, C., Reeuwijk, M., 2017. A neighbourhood-scale estimate for the cooling potential of green roofs. Urban Clim. 20, 33–45. https://doi.org/10.1016/j.uclim.2017.02.007

Tabares-Velasco, P.C., Srebric, J., 2012. A heat transfer model for assessment of plant based roofing systems in summer conditions. Build. Environ. 49, 310–323. https://doi.org/10.1016/j.buildenv.2011.07.019

Takane, Y., Ohashi, Y., Kusaka, H., Shigeta, Y., Kikegawa, Y., 2013. Effects of synoptic-scale wind under the typical summer pressure pattern on the mesoscale high temperature events in the Osaka and Kyoto urban areas by the WRF model. J. Appl. Meteorol. Climatol. 52, 1764–1778. https://doi.org/10.1175/JAMC-D-12-0116.1

Takebayashi, H., Moriyama, M., 2007. Surface heat budget on green roof and high reflection roof for mitigation of urban heat island. Build. Environ. 42, 2971–2979. https://doi.org/10.1016/j.buildenv.2006.06.017

Thomaier, S., Specht, K., Henckel, D., Dierich, A., Siebert, R.B., Freisinger, U.B., Sawicka,

M., 2014. Farming in and on urban buildings: present practice and specific novelties of Zero-Acreage Farming (ZFarming). Renew. Agric. Food Syst. 30, 43–54. https://doi.org/10.1017/S1742170514000143

Tsang, S.W., Jim, C.Y., 2011. Theoretical evaluation of thermal and energy performance of tropical green roofs. Energy 36, 3590–3598. https://doi.org/10.1016/j.energy.2011.03.072

Whittinghill, L.J., Rowe, D.B., Cregg, B.M., 2013. Evaluation of vegetable production on extensive green roofs. Agroecol. Sustain. Food Syst. 37, 465–484. http://dx.doi.org/10.1080/21683565.2012.756847

Whittinghill, L.J., Rowe, D.B., Andresen, J.A., Cregg, B.M., 2015. Comparison of stormwater runoff from sedum, native prairie, and vegetable producing green roofs. Urban Ecosyst. 18, 13–29. https://doi.org/10.1007/s11252-014-0386-8

Wong, G.K.L., Jim, C.Y., 2014. Quantitative hydrologic performance of extensive green roof under humid-tropical rainfall regime. Ecol. Eng. 70, 366–378. https://doi.org/10.1016/j.ecoleng.2014.06.025

Yaghoobian, N., Srebric., J., 2015. Influence of plant coverage on the total green roof energy balance and building energy consumption. Energy Build. 103, 1–13. https://doi.org/10.1016/j.enbuild.2015.05.052

Zhao, L., Lee, X., Smith, R.B., Oleson, K., 2014. Strong contributions of local background climate to urban heat islands. Nature 511 (7508), 216–219. doi:10.1038/nature13462

Wang, Y., Zacharias, J., 2015. Landscape modification for ambient environmental improvement in central business districts-A case from Beijing. Urban For. Urban Green. 14, 8–18. https://doi.org/10.1016/j.ufug.2014.11.005

Whittinghill, L.J., Rowe, D.B., Cregg, B.M., 2013. Evaluation of vegetable production on extensive green roofs. Agroecol. Sustain. Food Syst. 37, 465–484. http://dx.doi.org/10.1080/21683565.2012.756847

Whittinghill, L.J., Rowe, D.B., Andresen, J.A., Cregg, B.M., 2015. Comparison of stormwater runoff from sedum, native prairie, and vegetable producing green roofs.

Urban Ecosyst. 18, 13–29. https://doi.org/10.1007/s11252-014-0386-8

Wong, N.H., Chen, Y., Ong, C.L., Sia, A., 2003. Investigation of thermal benefits of rooftop garden in the tropical environment. Build. Environ. 38, 261–270. https://doi.org/10.1016/S0360-1323(02)00066-5

Wong, G.K.L., Jim, C.Y., 2014. Quantitative hydrologic performance of extensive green roof under humid-tropical rainfall regime. Ecol. Eng. 70, 366–378. https://doi.org/10.1016/j.ecoleng.2014.06.025

Wong, N.H., Jusuf, S.K., Win, A.A.L., Thu, H.K., Negara, T.S., Xuchao, W., 2007b. Environmental study of the impact greenery in an institutional campus in the tropics. Build. Environ. 42, 2949–2970. https://doi.org/10.1016/j.buildenv.2006.06.004

Wong, N.H., Tan, P.Y., Chen, Y., 2007a. Study of thermal performance of extensive rooftop greenery systems in the tropical climate. Build. Environ. 42, 25–54. https://doi.org/10.1016/j.buildenv.2005.07.030

Yaghoobian, N., Srebric., J., 2015. Influence of plant coverage on the total green roof energy balance and building energy consumption. Energy Build. 103, 1–13. https://doi.org/10.1016/j.enbuild.2015.05.052

Zhao, L., Lee, X., Smith, R.B., Oleson, K., 2014. Strong contributions of local background climate to urban heat islands. Nature 511 (7508), 216–219. doi:10.1038/nature13462

Zinzi, M., Agnoli, S., 2012. Cool and green roofs. An energy and comfort comparison between passive cooling and mitigation urban heat island techniques for residential buildings in the Mediterranean region. Energy Build. 55, 66–76. https://doi.org/10.1016/j.enbuild.2011.09.024

Publications

1. Yoshikazu Tanaka, Shigeto Kawashima, Takehide Hama, Luis Fernando Sánchez Sastre, Kimihito Nakamura, Yutaka Okumoto, 2016. Mitigation of heating of an urban building rooftop during hot summer by a hydroponic rice system, *Building and Environment* 96, 217–227.

2. Yoshikazu Tanaka, Shigeto Kawashima, Takehide Hama, Kimihito Nakamura, 2017. Thermal mitigation of hydroponic green roof based on heat balance, *Urban Forestry & Urban Greening* 24, 92–100.